AN ABSTRACT OF THE THESIS OF

Danielle E. Marias for the degree of Master of Science in Forest Ecosystems and Society presented on May 30, 2013.
Title: Impacts of Dwarf Mistletoe on the Physiology of Host *Tsuga heterophylla* Trees as Recorded in Tree Ring C and O Stable Isotopes

Abstract approved:

_____

Frederick C. Meinzer

Dwarf mistletoes, obligate, parasitic plants with diminutive aerial shoots, have long-term effects on host tree water relations, hydraulic architecture, and photosynthetic gas exchange and can eventually lead to tree death. To investigate the long-term impacts of dwarf mistletoe on gas exchange of host western hemlock trees, I compared growth, gas exchange, and tree-ring cellulose stable carbon and oxygen isotope ratios ($\delta^{13}C_{cell}$ and $\delta^{18}O_{cell}$) of heavily infected and uninfected trees. Relative basal area growth declined more rapidly with increasing tree size in infected than uninfected trees. Both radial growth and $\delta^{13}C_{cell}$ was significantly lower in infected than uninfected trees when trees were heavily infected. The combination of radial growth and $\delta^{13}C_{cell}$ patterns described the intensification of dwarf mistletoe throughout tree crowns through time.

$\delta^{13}C_{cell}$ and $\delta^{18}O_{cell}$ were significantly lower in infected trees than uninfected trees, an unexpected result given that stomatal conductance, relative humidity and other external variables expected to influence the $\delta^{18}O$ values of leaf water were

similar for infected and uninfected trees. Leaf mesophyll conductance (g_m) and effective pathlength (L) were estimated to explain observed differences in $\delta^{18}O_{cell}$ between infected and uninfected trees. Infected trees had significantly lower g_m and greater L than uninfected trees. These results point to the limitations of the dual isotope approach for identifying sources of variation in $\delta^{13}C_{cell}$ and indicate that changes in leaf internal properties such as L that affect $\delta^{18}O_{cell}$ must be considered. The significantly greater L and significantly lower g_m in infected compared to uninfected trees suggest that dwarf mistletoe may influence leaf structural and anatomical characteristics that are related to L and g_m.

Impacts of Dwarf Mistletoe on the Physiology of Host *Tsuga heterophylla* Trees as Recorded in Tree Ring C and O Stable Isotopes

by
Danielle E. Marias

A THESIS

submitted to

Oregon State University

in partial fulfillment of
the requirements for the
degree of

Master of Science

Presented May 30, 2013
Commencement June 2014

Master of Science thesis of Danielle E. Marias presented on May 30, 2013.

APPROVED:

_____

Major Professor, representing Forest Ecosystems and Society

_____

Head of the Department of Forest Ecosystems and Society

_____

Dean of the Graduate School

I understand that my thesis will become part of the permanent collection of Oregon State University libraries. My signature below authorizes release of my thesis to any reader upon request.

_____

Danielle E. Marias, Author

ACKNOWLEDGEMENTS

First, I would like to thank my advisor Rick Meinzer for providing invaluable guidance and support throughout this project. Your insight, creativity, and wisdom are inspiring and motivating. Dave Shaw, I appreciate our great discussions about dwarf mistletoe, your enthusiasm, and help in the field. Dave Woodruff, thank you for allowing me to expand on your previous work that laid the foundation for this project as well as your assistance in the field. Barb Lachenbruch, thank you for your willingness to serve as a committee member and comments on the project. I am grateful for contributions from Renée Brooks and Steve Voelker for being role models and sharing their expertise in isotopes, tree rings, and data interpretation. I also thank Jennifer McKay for being accommodating and helpful with isotope samples. I would like to thank Kristen Falk and Brandy Saffell for their assistance in the lab and field, especially those late nights of cellulose extractions. Most of all, thank you to my family for their continued support through my educational journey and your role as the rock in my life. I am very grateful for an amazing community of friends and colleagues in the College of Forestry who have been incredibly generous and encouraging through stimulating discussions and advice, as well as distractions from work when I needed it most.

CONTRIBUTION OF AUTHORS

Chapter 2: Frederick C. Meinzer, David R. Woodruff, David C. Shaw, Steven L. Voelker, J. Renée Brooks, and Barbara Lachenbruch provided guidance in analysis, writing, and editing. Kristen Falk and Jennifer McKay provided assistance in field and lab work.

TABLE OF CONTENTS

LIST OF FIGURES

LIST OF TABLES

Impacts of Dwarf Mistletoe on the Physiology of Host *Tsuga heterophylla* Trees as Recorded in Tree Ring C and O Stable Isotopes

1. INTRODUCTION

Parasitic angiosperms are widespread and can be found throughout the world in most ecosystems from subarctic tundra to tropical forests (Bell & Adams, 2010). More than 3000 plant species distributed over 18 families rely on a parasitic association with a host plant for nutrient, water, and carbon supply (Lambers *et al.*, 2008, p. 445). Parasitic plants are distinguished as facultative parasites when they can grow to maturity without a host, or as obligate parasites when they require a host to reach maturity. In addition, holoparasites lack chlorophyll and require water and nutrients from their host, while hemiparasites contain chlorophyll but still may require water and nutrients from their host; however, the distinction between types is not sharp (Lambers *et al.*, 2008, p. 445). Parasitic plants are categorized into aerial parasites that infect stems (40% of all species) and root parasites (60% of all species) (Bell & Adams, 2012).

Dwarf mistletoes (*Arceuthobium* spp., Viscaceae in the Santales order) are aerial, obligate, hemiparasitic plants that infect conifers throughout North America as well as around the world (Geils *et al.*, 2002). The genus *Arceuthobium* has 42 species of dwarf mistletoe (36 species according to Nickrent 2002) that are host-specific often with primary or secondary hosts (Geils *et al.*, 2002). Dwarf mistletoe has been considered a destructive pathogen of commercially valuable conifers in regions of the United States and Mexico because it has detrimental impacts on host trees resulting in significant ecological effects and economic losses (Korstian & Long 1922; Hawksworth & Shaw, 1984). Dwarf mistletoes are known to reduce radial growth

(Stanton, 2007; Shaw *et al.,* 2008; Logan *et al.,* 2012) and induce branch deformation and dieback, and tree death.

Dwarf mistletoes are in the same family (Viscaceae) as leafy mistletoes (popular around Christmas time) of the genera *Viscum* and *Phoradendron*; however, dwarf mistletoes differ considerably from "true" or leafy mistletoes because they have diminutive, leafless aerial shoots and a miniscule transpiring shoot area compared to leafy mistletoes, which are considered to be significant water parasites (Marshall *et al.,* 1994a, b; Zweifel *et al.,* 2012; Mathiasen *et al.,* 2008). The majority of published studies on the effects of mistletoes on host physiology have focused on leafy mistletoes. Because of the substantial differences in size and shoot morphology between dwarf and leafy mistletoes, their impacts on host function are likely to differ, suggesting that the results of ecophysiological studies on leafy mistletoes may not be applicable to dwarf mistletoes.

Dwarf mistletoes have a complex life history that spans a range of temporal and spatial scales (Hawksworth & Wiens, 1972; 1996). They are dioecious and produce nectar-bearing flowers. After pollination, fruits take 13-14 months to mature. Seeds are explosively discharged from hydrostatic pressure up to 15 m from a single-seeded berry, causing dwarf mistletoe populations to be clumped based on stand structural attributes such as tree and crown density and mistletoe position (Hawksworth & Wiens, 1996). The local light environment and canopy density influence dwarf mistletoe occurrence (Bickford *et al.,* 2005) and location of infection centers (Shaw *et al.,* 2005). Viscin, a sticky seed coating, enables seeds to adhere to

conifer needles and slide to the base of the needle. Once attached to a branch, the seed establishes a holdfast structure to develop strands and sinkers of its endophytic system and haustorial connections with host phloem and xylem (Hawksworth & Wiens, 1996).

Localized branch infections induced by dwarf mistletoe are visible as spindle-shaped swellings (Geils *et al.,* 2002). Diminutive, leafless aerial shoots erupt from these swellings approximately 2-7 years after seed germination and flower production occurs in another 1-2 years (Geils *et al.,* 2002). Dwarf mistletoes can survive within the host without aerial shoots as “cryptic infections” because they acquire carbohydrates from the host and reproductive success does not require annual seed production (Robinson & Geils, 2006). Downstream from swellings, the host tree forms dense, fan-shaped branching systems called 'witches' brooms' that develop over a period of several years to decades. Witches’ broom formations have been associated with transient increases in radial growth due to the transient increase in leaf area (Sala *et al.,* 2001; Stanton, 2007) and perturbations in growth regulating hormones such as cytokinins. Needles on branches of host white spruce (*Picea glauca*) infected with *A. pusillum* had 79% greater cytokinin content than uninfected branches (Logan *et al.,* 2012). Eventually, disruption of xylem water transport and diversion of host resources by dwarf mistletoe leads to needle loss and branch dieback (Meinzer *et al*., 2004).

Dwarf mistletoes are host-specific parasites, although some have primary and secondary hosts (Geils *et al.,* 2002). Their success is highly correlated with host tree vigor (Bickford *et al.,* 2005; Stanton, 2007; Sanguesa-Barreda *et al*., 2012). Maloney

and Rizzo (2002) found that the dwarf mistletoe rating (DMR), a measure of infection severity, was positively correlated with host white fir (*Abies concolor*) size. Watson (2008) proposed the "host-quality hypothesis" in which the occurrence of parasitic plants is nonrandom and is related to host tree access to water, nutrients, or other resources that can be limiting to hosts. Therefore, parasites are more likely to establish and survive on trees with greater access to these resources.

Although the life history of dwarf mistletoes is well understood and has been thoroughly studied, challenges remain in quantifying their effects on host physiology, as well as estimating when trees were initially infected. In addition, the extent of dwarf mistletoe on a landscape scale has not been adequately quantified, primarily because it is difficult to detect during aerial surveys (Hennon *et al.,* 2011). However, a range of approaches have been used to understand functional relationships, differences, and similarities between leafy mistletoes and dwarf mistletoes and their woody hosts (Bell & Adams, 2010). These include measurements of physiological variables such as stomatal conductance, transpiration, respiration, photosynthesis, and sap flow; tracer experiments using isotopes such as ^{15}N, ^{13}C, and ^{18}O of xylem sap, leaf tissue, and leaf water; and spectroscopic studies of minerals and solutes (Hull & Leonard 1964; Goldstein *et al.,* 1989; Flanagan *et al.,* 1993; Marshall *et al.,* 1994a, b; Cernusak *et al.,* 2004; Urban *et al.,* 2012; Lu *et al.,* 2013). These measurements are sufficient for relatively short time scales and can shed light on the physiology of the host-parasite relationship close to or at the time of the measurement. However, estimating when trees were initially infected is particularly difficult because host trees

can be infected without visible signs of infection during the latency phase. In addition, progression of the dwarf mistletoe infection and broom formation occurs over decades. The rate of change in infection severity is anecdotally estimated to be an increase of one DMR class per decade (Geils & Mathiasen, 1990; DC Shaw, *personal communication*). Epidemiological simulation models have been developed to estimate how fast the infection increases, although these models are limited by geographic range and species and still need to be further developed, calibrated, and validated (Robinson & Geils, 2006). The need for a way to estimate initial timing of infection, and to detect the progression of the infection through time, inspired one of the goals of this thesis research.

Of the few studies that focus on dwarf mistletoe effects on the physiology of host trees, results are conflicting due to the differing interactions between different species of dwarf mistletoes and hosts. For example, Sala *et al*. (2001) found that leaf area:sapwood area ratios (A_L:A_S) of host Douglas-fir (*Pseudotsuga menziesii*) infected with *A. douglasii* were greater than in uninfected trees although A_L:A_S did not differ significantly between host western larch (*Larix occidentalis*) infected with *A. laricis* and uninfected trees. Leaves on host western hemlock (*Tsuga heterophylla*) branches infected with *A. tsugense* had significantly lower photosynthetic capacity than those on uninfected trees (Meinzer *et al.,* 2004). In contrast, photosynthetic capacity did not differ between leaves on host white spruce branches (*Picea glauca*) branches infected and uninfected with *A. pusillum* (Logan *et al.,* 2002). However, all three studies (Sala *et al.,* 2001; Meinzer *et al.,* 2004; Logan *et al.,* 2012) found that needles of infected

branches had significantly more negative carbon stable isotope ratios ($\delta^{13}C$) than uninfected branches. Infected western hemlock displayed lower whole tree water use than uninfected trees in the Wind River Experimental Forest in southwestern Washington (Meinzer *et al.,* 2004) while infected Douglas-fir and infected western larch in the Rocky Mountains of the Lolo National Forest in Missoula, Montana did not display significantly different whole tree water use than uninfected trees (Sala *et al.,* 2001). These conflicting findings across and within studies emphasize the challenges to fully understand the effects of dwarf mistletoes on host physiology. The varying results may occur because *A. pusillum* and *A. douglasii* produce "systemic" infections where dwarf mistletoe infects the meristems of host trees and grows in concert with branches resulting in very large witches' brooms. In contrast, *A. tsugense* and *A. laricis* produce "local" infections that produce smaller witches' brooms. Clearly, contrasting results indicate that the physiological effects of dwarf mistletoes on their hosts remain unresolved and vary across combinations of dwarf mistletoe-host species.

Another challenge to understanding the physiological effects of dwarf mistletoe on its host is that most ecophysiological studies have focused on leafy mistletoes (Goldstein *et al.,* 1989; Flanagan *et al.,* 1993; Marshall *et al.,* 1994a, b; Tennakoon & Pate, 1996; Cernusak *et al.,* 2004; Wang *et al.,* 2007; Zweifel *et al.,* 2012). However, dwarf mistletoes differ considerably from leafy mistletoes in aerial shoot size and morphology and likely in their effects on host physiology. Dwarf mistletoes have diminutive, essentially leafless aerial shoots. Therefore, dwarf

mistletoes are more heterotrophic (Hull & Leonard, 1964b; Logan *et al.*, 2002) and have a miniscule transpiring shoot area compared to leafy mistletoes, which are considered to be significant water parasites because of their high transpiration rate per unit leaf area relative to that of the host tree (Marshall *et al.*, 1994a, b; Zweifel *et al.*, 2012). As a result, long-term negative impacts of dwarf mistletoes on tree growth and carbon balance are likely to be indirect and related to disruption of water transport and consequent alterations in hydraulic architecture and photosynthetic gas exchange, rather than directly related to interception of water and fixed carbon seen with leafy mistletoe. Differences in shoot size and morphology cause studies of leafy mistletoes to be less informative for understanding functional relationships between hosts and dwarf mistletoes.

To better understand the physiology of host-parasitic plant relationships, ecophysiological studies have employed stable isotope analyses that integrate tree physiological responses over time and space. Carbon (C), oxygen (O), and nitrogen (N) isotope ratios of aerial shoots, leaf tissue, leaf water, xylem sap, and tree rings have been used to investigate the functional relationships between forest pathogens and woody hosts (Hull & Leondard, 1964; Goldstein *et al.*, 1989; Flanagan *et al.*, 1993; Marshall *et al.*, 1994a, b; Wang *et al.*, 2007; Simard *et al.*, 2012). Studies have used C isotope ratios in plant tissues and xylem water to track movement of C and nutrients from host to parasite while others have used O isotope ratios of leaf water of host and parasite to compare transpiration rates. However, most studies have focused on leafy mistletoes and few have used isotopes to compare uninfected and infected

hosts (versus comparing host and parasitic plant). Studies using isotopes have shown that *Phoradendron* (a leafy mistletoe) and *Arceuthobium* have different effects on host physiology. Hull & Leonard (1964) tracked the subsequent translocation and accumulation of isotopically-labeled photosynthate to compare *Arceuthobium* and *Phoradendron* effects. They found that *Arceuthobium* accumulated significant host photosynthate in its endophytic system and aerial shoots while *Phoradendron* did not. This supported the long-held perspective that leafy mistletoes are primarily water parasites while dwarf mistletoes acquire both water and carbon from host trees. However, more recent studies have shown that xylem-tapping mistletoes, which do not access host phloem, acquire C dissolved in host photosynthate and xylem water. Wang *et al*. (2007) found that mistletoes derived 34%-77% of their carbon from host photosynthate depending on species and locations along a semi-arid transect, whereas Marshall *et al*. (1994b) found that heterotrophic C gain derived from host xylem sap represented 15% of total C gain. This is consistent with findings that high transpiration rates of mistletoes relative to hosts allow for rapid import of solutes including C and N via xylem water (Schulze *et al*., 1984; Goldstein *et al.*, 1989; Marshall *et al.*, 1994a, b; Lambers *et al.*, 2008, p. 453). Higher transpiration rates were consistent with lower $\delta^{18}O$ values of leafy mistletoe (*Amyema miquelii, Amyema preissii*) leaf tissue compared to host (*Eucalyptus wandoo, Acacia acuminate*) tissue (Cernusak *et al.*, 2004). As a result of higher transpiration rates and lower photosynthetic rates of mistletoes relative to hosts, mistletoes have lower intrinsic water use efficiency (WUE), defined as the ratio of the CO_2 assimilation rate to stomatal conductance

(A/g_s,) and greater ^{13}C isotope discrimination than their hosts (Goldstein *et al.,* 1989; Marshall *et al.,* 1994a; Cernusak *et al.,* 2004; Wang *et al.,* 2007; Lambers *et al.,* 2008, p. 453). Lower photosynthetic rates have been attributed to the low concentration of *N* dissolved in host xylem water (Ehleringer *et al.,* 1985; Schulze *et al.,* 1991). High transpiration rates of mistletoes have been shown to significantly influence host gas exchange. Zweifel *et al*., (2012) found that host Scots pine (*Pinus sylvestris*) infected with *Viscum album* compensated for *V. album's* lack of stomatal regulation and high transpiration rates by closing its own stomata. Despite reduced stomatal aperture of host needles, total water loss of infected branches was still higher than uninfected branches, causing mistletoe to be referred to as a "leak" in the host water transport system. In addition, reduced host stomatal aperture reduced water loss but also reduced C gain. The abundance of studies that investigate leafy mistletoe physiology suggests that high transpiration rates have significant effects on host water relations that likely differ from dwarf mistletoes.

Because of differences in shoot size and morphology, the effects of dwarf mistletoes and leafy mistletoes on host physiology are likely not comparable, emphasizing the need for more studies of dwarf mistletoes and their impacts on host physiology. It is likely that dwarf mistletoes acquire a greater percent of their total C from hosts than leafy mistletoes due to their small, leafless shoots; however, the overall demand for C and water by dwarf mistletoes on hosts likely is smaller than their larger, leafier relatives. The diminutive shoots have a thick cuticular layer that reduce water loss and thus transpiration, suggesting that dwarf mistletoes may have

the ability to regulate gas exchange (Calvin & Wilson, 1996), contrary to leafy mistletoes that are considered to have high, unregulated transpiration rates (Zweifel *et al.,* 2012). Reduced water loss would likely also reduce C gain through stomata, suggesting that dwarf mistletoes are more heterotrophic and acquire a greater percent of C from hosts than leafy mistletoes (Hull & Leonard, 1964). In addition to a thick cuticular layer, other characteristics of dwarf mistletoe shoots that may reduce transpiration include low external surface to volume ratio, sunken guard cells, small substomatal chambers, and lack of intercellular space in mesophyll tissue (Calvin & Alosi, 1983).

Stable isotopes in tree rings can be a useful tool for addressing the challenges to understanding the host-dwarf mistletoe functional relationship through time. Stable isotopes of tree ring cellulose are used to reconstruct past climate and infer tree physiological responses to climate because tree rings annually record and integrate the impacts of physiology and the environment at the time the ring was formed (McCarroll & Loader, 2004). Studies have shown that C and O isotopic ratios in tree ring cellulose ($\delta^{13}C_{cell}$ and $\delta^{18}O_{cell}$) provide valuable information about plant C and water relations (Saurer *et al.,* 1997; Barnard *et al.,* 2012) and past environmental conditions (Roden *et al.,* 2000; Brooks & Mitchell, 2011). Since products of photosynthesis (*A*) are exported from the leaf and converted to cellulose to form tree rings, the $\delta^{13}C$ signal of the leaf is imprinted in the $\delta^{13}C_{cell}$ of tree rings (Leavitt & Long, 1982) and reflects leaf gas exchange by the tree at the time the C was fixed. Therefore, the $\delta^{13}C$ of tree rings provides information about gas exchange parameters

including photosynthetic capacity (A_{max}) and the conductance (g) to CO_2 entering the leaf to sites of carboxylation in the chloroplast. Conductance to CO_2 from the atmosphere into the leaf and then into the mesophyll where chloroplasts are located, is influenced by stomatal conductance (g_s) and mesophyll conductance (g_m), respectively (Evans *et al.*, 2009). Because water and CO_2 passing in and out of the leaf have overlapping pathways (Ferrio *et al.*, 2012; Flexas *et al.*, 2012), $\delta^{13}C_{cell}$ of tree rings is often used as a measure of intrinsic water use efficiency (WUE) defined as A/g_s. The O isotope ratio of plant cellulose, $\delta^{18}O_{cell,}$ has been shown to be useful for separating variation in A and g_s because the $\delta^{18}O_{cell}$ is only influenced by the water cycle, including g_s but not A (Scheidegger *et al.*, 2000). However, this approach ignores g_m, although it can significantly influence $\delta^{18}O$ of leaf water and thus $\delta^{18}O_{cell}$. G_m has been linked to photosynthesis under ambient conditions (Woodruff *et al.*, 2009) and to A_{max} (Flexas *et al.*, 2012). The $\delta^{18}O_{cell}$ is influenced by the isotopic composition of source water, atmospheric water vapor, evaporative enrichment of leaf water (Roden *et al.*, 2000; Barbour, 2007) and g_s.

In this study, I used $\delta^{13}C_{cell}$ and $\delta^{18}O_{cell}$ to infer past climate (precipitation, relative humidity, vapor pressure deficit) and tree physiology (A_{max}, g_s). With known C and O isotopic compositions of atmospheric CO_2 and precipitation; or by comparing treatment groups in the same stand experiencing similar sources of C and O, I can use $\delta^{13}C_{cell}$ and $\delta^{18}O_{cell}$ to infer shifts in A_{max} and g_s. However, shifts in A_{max} and g_s that are recorded by $\delta^{13}C_{cell}$ and $\delta^{18}O_{cell}$ of tree rings reflect not only tree responses to

environmental conditions, but also tree responses to pathogens that may influence tree gas exchange. Consequently, interpretations of tree ring stable isotope signals can be confounded by interacting tree responses to climate and forest pathogens. Therefore, studies using tree ring stable isotopes to reconstruct past climate and tree responses to climate should use caution and recognize that forest pathogens can have substantial effects on isotopic signals that may complicate interpretations of the isotopic composition of tree rings if the pathogen is undetected.

With careful study design (e.g. accounting for differences in environmental conditions and inherent differences in physiology across species), tree ring stable isotopes can be used to detect effects of pathogens on host physiology, as well as when the "signatures" of pathogens may have become present in the tree ring record. Haavik *et al*. (2007) used $\delta^{13}C_{cell}$ of tree rings to investigate the effects of red oak borer (*Enaphalodes rufulus*) that feeds on phloem tissue of northern red oak (*Quercus rubra*). Simard *et al*. (2012) used both $\delta^{13}C_{cell}$ and $\delta^{18}O_{cell}$ of tree rings to detect the presence of past outbreaks of spruce budworm (*Choristoneura fumiferana*) that defoliate balsam fir (*Abies balsamea*). They found no differences in photosynthesis or stomatal conductance between treatment groups and attributed higher $\delta^{13}C_{cell}$ in defoliated trees to the mobilization of carbohydrate reserves that have higher $\delta^{13}C$ values compared to recent assimilates. Injury to host trees by insects occurs by feeding on phloem tissue and defoliation. In contrast, injury to host trees by dwarf mistletoe is not caused by a physical girdle (Hull & Leonard, 1964) and needle loss likely occurs

as a compensatory mechanism to maintain leaf-specific conductivity in response to reduced branch hydraulic conductivity due to physical obstruction by dwarf mistletoe (Meinzer *et al.*, 2004). Sanguesa-Barreda *et al*. (2012) used tree ring $\delta^{13}C_{cell}$ to investigate the effects of the nutrient and water demands of leafy mistletoe *Viscum album* on radial growth and WUE of host Scots pine. Unlike leafy mistletoes and insects, dwarf mistletoes have more indirect, long-term, cumulative effects that progress over decades likely due to their complex life history and diminutive size relative to host tree size.

To my knowledge, this thesis research is the first study to use both $\delta^{13}C_{cell}$ and $\delta^{18}O_{cell}$ of tree rings to investigate the effects of a parasitic plant on host physiology through time. I compared annual radial growth, $\delta^{13}C_{cell}$, and $\delta^{18}O_{cell}$ of co-occurring uninfected and infected old-growth western hemlock trees in southwestern Washington to evaluate the utility of the dual isotope ($\delta^{13}C_{cell}$ and $\delta^{18}O_{cell}$) approach and the long-term effects of the infection on host photosynthetic gas exchange. Based on previous measurements of photosynthetic gas exchange and leaf-specific hydraulic conductivity (Meinzer *et al.*, 2004), I expected infected trees to have reduced radial growth, lower $\delta^{13}C_c$, and similar $\delta^{18}O_{cell}$ to uninfected trees.

REFERENCES

Barbour MM. 2007. Stable oxygen isotope composition of plant tissue: a review. *Functional Plant Biology* **34**: 83–94.

Barnard HR, Brooks JR, Bond BJ. 2012. Applying the dual-isotope conceptual model to interpret physiological trends under uncontrolled conditions. *Tree Physiology* **32**: 1183-1198.

Bell TL, Adams MA. 2011. Attack on all fronts: functional relationships between aerial and root parasitic plants and their woody hosts and consequences for ecosystems. *Tree Physiology* **31**:3-15.

Bickford CP, Kolb TE, Geils BW. 2005. Host physiological condition regulates parasitic plant performance: *Arceuthobium vaginatum* subsp. *cryptopodum* on *Pinus ponderosa*. *Oecologia* **146**: 179–189.

Brooks JR, Mitchell AK. 2011. Interpreting tree responses to thinning and fertilization using tree-ring stable isotopes. *New Phytologist* 190: 770-782.

Calvin CL, Alosi MC. 1983. Developmental anatomy of the epidermis of the dwarf mistletoe *Arceuthobium tsugense*. *American Journal of Botany* 70.

Cernusak, Lucas A., John S. Pate, and Graham D. Farquhar. 2004. Oxygen and carbon isotope composition of parasitic plants and their hosts in southwestern Australia. *Oecologia* 139: 199-213.

Ehleringer JR, Schulze ED, Ziegler H, Lange OL, Farquhar GD, Cowan IR. 1985. Xylem-tapping mistletoes: water or nutrient parasites. *Science* 227: 1479-1481.

Evans JR, Kaldenhoff R, Genty B, Terashima I. 2009. Resistances along the CO2 diffusion pathway inside leaves. *Journal of Experimental Botany* 60: 2235-2248.

Ferrio JP, Pou A Florez-Sarasa I, Gessler A, Kodama N, Flexas J, Ribas-Carbo M. 2012. The Péclet effect on leaf water enrichment correlates with leaf hydraulic conductance and mesophyll conductance for CO2. *Plant, Cell & Environment* 35: 611-625.

Flanagan LB, Marshall JD, Ehleringer JR. 1993. Photosynthetic gas exchange and the stable isotope composition of leaf water: comparison of a xylem-tapping mistletoe and its host. *Plant, Cell & Environment* 16: 623-631.

Flexas J, Barbour MM, Brendel O, Cabrera HM, Carriquí M, Diaz-Espejo A, Douthe C, Dreyer E, Ferrio JP, Gago J, Galle A, Galmes J, Kodama N, Medano H, Niinemets U, Pequero-Pina JJ, Pou A, Ribas-Carbo M, Tomas M, Tosens T, Warren CR. 2012. Mesophyll diffusion conductance to CO2: An unappreciated central player in photosynthesis. *Plant Science* 196: 70-84.

Giels BW, Mathiasen RL. 1999. Intensification of Dwarf Mistletoe on Southwestern Douglas-fir. *Forest Science* 36: 955-969.

Geils BW, Tovar JC, Moody B. **2002**. Mistletoes of North American Conifers. General Technical Report RMRS-GTR-98.

Goldstein GF, Rada L, Sternberg JL, Burguera M, Burguera A, Orozco M, Montilla M, Zabala O, Azocar A, Canales MJ, Ceils A. 1989. Gas exchange and water balance of a mistletoe species and its mangrove hosts. *Oecologia* 78: 176-183.

Haavik LJ, Stephen FM, Fierke MK, Salisbury VB, Leavitt SW, Billings SA. 2007. Dendrochronological parameters of norther red oak infested with red oak borer. *Forest Ecology and Management* 255:1501-1509.

Hawksworth, FG, Wiens D. 1972. Biology and classification of dwarf mistletoes (*Arceuthobium*). USDA Agriculture Handbook 401. Washington, DC: USDA Forest Service, 234 pp.

Hawksworth, FG, Shaw CG III. 1984. Damage and loss caused by dwarf mistletoes in coniferous forests of western North America. Pages 285-297 in R. K. S. Wood and G. J. Jellis, editors. Plant diseases: infection, damage, and loss. Blackwell Scientific, Oxford, England.

Hawksworth, FG, Wiens D. 1996. Dwarf mistletoes: Biology, pathology and systematics. Agriculture Handbook 709. Washington, DC: USDA Forest Service, 410 pp.

Hennon, P, Barrett TM, Wittwer D. 2011. "The distribution of hemlock dwarf mistletoe suggests influences of climate," *Forests of Southeast and South-Central Alaska, 2004-2008*.
Gen. Tech. Rep. PNW-GTR-835. Portland, OR: U.S. Department of Agriculture, Forest Service, Pacific Northwest Research Station, pp. 74-77.

Hull RJ, Leonard OA. 1964. Physiological aspects of parasitism in mistletoes (Arceuthobium and Phoradendron). I. The carbohydrate nutrition of mistletoe. *Plant Physiology* 39: 996-1007.

Korstian CF, Long WH. 1922. The western yellow pine mistletoe: Effect on growth and suggestions for control. US Dept. Agr. Bul. 1112, 35 pp.

Lambers H, Chapin FS, Chapin FS, Pons TL. 2008. *Plant physiological ecology*. New York, US: Springer.

Leavitt SW, Long A. 1982. Evidence for 13C/12C fractionation between tree leaves and wood. *Nature* 298: 742-744.

Logan BA, Huhn ER, Tissue DT. 2002. Photosynthetic characteristics of eastern dwarf mistletoe (*Arceuthobium pusillum* Peck) and its effects on the needles of host white spruce (*Picea glauca* [Moench] Voss). *Plant Biology* 4: 740-745.

Logan BA, Reblin JS, Zonana DS, Dunlavey RF, Hricko CR, Hall AW, Schmiege SC, Buschek RA, Duran KL, Neil Emery RJ, Kurepin LV, Lewis JD, Pharis RP, Phillips NH, Tissue DT. 2012. Impact of eastern dwarf mistletoe (*Arceuthobium pusillum*) on host white spruce (*Picea glauca*) development, growth and performance across multiple scales. *Physiologia Plantarum* 147: 502–513.

Lu K, Kang LH, Sprent JI, Xu DP, He XH. 2013. Two-way transfer of nitrogen between *Dalbergia odorifera* and its hemiparasite *Santalum album* is enhanced when the host is effectively nodulated and fixing nitrogen**.** *Tree Physiology* 00: 1-11.

Maloney PE, Rizzo DM. 2002. Dwarf mistletoe-host interactions in mixed-conifer forests in the Sierra Nevada. *The American Phytopathological Society* 92: 597-602.

Marshall JD, Dawson TE, Ehleringer JR. 1994a. Integrated nitrogen, carbon, and water relations of a xylem-tapping mistletoe following nitrogen fertilization of the host. *Oecologia* 100: 430-438.

Marshall JD, Ehleringer JR, Schulze ED, Farquhar G. 1994b. Carbon isotope composition, gas exchange and heterotrophy in Australian mistletoes. *Functional Ecology* 8: 237-241.

Mathiasen RL, Nickrent DL, Shaw DC, Watson DM. 2008. Mistletoes: Pathology, Systematics, Ecology, and Management. *The American Phytopathological Society* 92: 988-1006.

McCarroll D, Loader NJ. 2004. Stable isotopes in tree rings. *Quarternary Science Reviews* 23:771-801.

Meinzer FC, Woodruff DR, Shaw DC. 2004. Integrated responses of hydraulic architecture, water and carbon relations of western hemlock to dwarf mistletoe infection. *Plant, Cell and Environment* 27:937-946.

Nickrent DL. 2002. Mistletoe phylogenetics: Current relationships gained from analysis of DNA sequences. Pp. 48-57 in: Proceedings of the Western International Forest Disease Work Conference, August 14-18, 2000. Waikoloa, Hawai'i. 253 pp.

Robinson DCE, Geils BW. 2006. Modeling dwarf mistletoe at three scales: life history, ballistics and contagion. *Ecological Modeling* 4431: 1-16.

Roden JS, Lin G, Ehleringer JR. 2000. A mechanistic model for interpretation of hydrogen and oxygen isotope ratios in tree-ring cellulose. *Geochimica et Cosmochimica Acta* 64: 21–35.

Sala A, Carey EV, Callaway RM. 2001. Dwarf mistletoe affects whole-tree water relations of Douglas fir and western larch primarily through changes in leaf to sapwood ratios. *Oecologia* 126: 42-52.

Sanguesa-Barreda G, Linares JC, Camarero JJ. 2013. Drought and mistletoe reduce growth and water-use efficiency of Scots pine. *Forest Ecology and Management* 296: 64-73.

Saurer M, Aellen K, Siegwolf R. 1997. Correlating δ13C and δ18O in cellulose of trees. *Plant, Cell & Environment* 20: 1543-1550.

Scheidegger Y, Saurer M, Bahn M, Siegwolf R. 2000. Linking stable oxygen and carbon stable isotopes with stomatal conductance and photosynthetic capacity: a conceptual model. *Oecologia* 125: 350-357.

Schulze ED, Turner NC, Glatzel G. 1984. Carbon, water and nutrient relations of two mistletoes and their hosts: A hypothesis. *Plant, Cell and Environment* 7: 293-299.

Schulze ED, Lange OL, Zeigler H, Gebauer G. 1991. Carbon and nitrogen isotope ratios of mistletoes growing on nitrogen and non-nitrogen fixing hosts and on CAM plants in the Namib desert confirm partial heterotrophy. *Oecologia* 88: 457-462.

Shaw DC, Chen J, Freeman EA, Braun DM. 2005. Spatial and population characteristics of dwarf mistletoe infected tree sin an old-growth Douglas-fir – western hemlock forest. *Canadian Journal of Forest Research* 35: 990-1001.

Shaw DC, Huso M, Bruner H. 2008. Basal area growth impacts of dwarf mistletoe on western hemlock in an old-growth forest. *Canadian Journal of Forest Research* 38: 576-583.

Simard S, Morin H, Krause C, Buhay WM, Treydte K. 2012. Tree-ring widths and isotopes of artificially defoliated balsam firs: A simulation of spruce budworm outbreaks in Eastern Canada. *Environmental and Experimental Botany* 81: 44-54.

Stanton S. 2007. Effects of dwarf mistletoe on climate response of mature ponderosa pine trees. *Tree-Ring Research* 63: 69-80.

Tennakoon, K. U., & Pate, J. S. (1996). Effects of parasitism by a mistletoe on the structure and functioning of branches of its host. *Plant, Cell & Environment*, *19*(5), 517-528.

Urban J, Gebaurer R, Nadezhdina N, Cermak J. 2012. Transpiration and stomatal conductance of mistletoe (*Loranthus europaeus*) and its host plant, downy oak (*Quercus pubescence*). Biologia 67:917-926.

Wang L, Kgobe B, D'Odorico P, Macko SA. 2007. Carbon and nitrogen parasitism by a xylem-tapping mistletoe (Tapinanthus oleifolius) along the Kalahari Transect: a stable isotope study. *African Journal of Ecology* 46: 540-546.

Watson DM. 2008. Determinants of parasitic plant distribution: the role of host quality. *Botany* 87: 16-21.

Woodruff DR, Meinzer FC, Lachenbruch B, Johnson DM. 2009. Coordination of leaf structure and gas exchange along a height gradient in a tall conifer. *Tree Physiology*, 29: 261–272.

Zweifel R, Bangerter S, Rigling A, Sterck FJ. 2012. Pine and mistletoes: how to live with a leak in the water flow and storage system? *Journal of Experimental Botany* 63: 2565-2578.

2. IMPACTS OF DWARF MISTLETOE ON THE PHYSIOLOGY OF HOST *TSUGA HETEROPHYLLA* TREES AS RECORDED IN TREE RING C AND O STABLE ISOTOPES

Danielle E. Marias, Frederick C. Meinzer, David R. Woodruff, David C. Shaw, Steven L. Voelker, J. Renée Brooks, Barbara Lachenbruch, Kristen Falk, Jennifer McKay

INTRODUCTION

Dwarf mistletoe (*Arceuthobium* spp. Viscaceae) is an obligate, parasitic plant that primarily infects coniferous species. It is considered to be extremely destructive because it may eventually induce host tree death once a host tree is infected. Similar to leafy mistletoes of the Loranthaceae and other families, dwarf mistletoes acquire carbohydrates, nutrients, and water almost completely from host trees through haustorial connections to host xylem and phloem (Hawksworth & Wiens, 1996). However, dwarf mistletoes differ considerably from leafy mistletoes because they have diminutive aerial shoots that are essentially leafless. Therefore dwarf mistletoes are more heterotrophic (Hull & Leonard, 1964; Logan *et al.*, 2002) and have a miniscule transpiring shoot area compared to leafy mistletoes. Leafy mistletoes are considered to be significant water parasites because of their high transpiration rate per unit leaf area relative to that of the host tree (Marshall *et al.*, 1994a, b; Zweifel *et al.*, 2012).

As a result, long-term negative impacts of dwarf mistletoes on tree growth and carbon balance are likely to be indirect and related to disruption of water transport and consequent alterations in hydraulic architecture and photosynthetic gas exchange rather than directly related to interception of water and fixed carbon. Water use of western hemlock (*Tsuga heterophylla*) trees heavily infected with dwarf mistletoe (*A. tsugense*) was substantially less than that of co-occurring uninfected trees of similar size because of branch dieback and reduced leaf area on surviving infected branches

(Meinzer *et al.*, 2004). Needle shedding on infected western hemlock branches conserved their leaf-specific conductivity despite sharply reduced hydraulic conductivity in spindle-shaped branch swellings (Meinzer *et al.*, 2004). The predictable scaling of stomatal conductance (g_s) and photosynthesis (A) with leaf-specific conductivity (Hubbard *et al.*, 2001; Santiago *et al.*, 2004) suggests that photosynthetic gas exchange characteristics may be similar in needles on infected and uninfected trees. However, Sala *et al*. (2001) and Meinzer *et al*. (2004) observed reduced host leaf nitrogen (N) content, photosynthetic capacity (A_{max}), and intrinsic water use efficiency (WUE; defined as the ratio A/g_s) in coniferous trees infected with dwarf mistletoe. These dwarf mistletoe-induced alterations in photosynthetic gas exchange were recorded in stable carbon isotope ratios of needles on infected western hemlock branches (Meinzer *et al.*, 2004).

Because dwarf mistletoe infections are initially localized and increase in severity over several decades, estimating when trees were initially infected and evaluating host physiological responses to the infection through time is difficult (Geils *et al.*, 2002). Past growth responses of trees and their underlying physiological basis can often be characterized by concurrent analyses of tree-ring widths and stable isotopes of tree ring cellulose which record and integrate the impacts of physiology and the environment at the time the ring was formed (McCarroll & Loader, 2004). Since tree ring growth is inherently variable and provides limited information about tree physiology, stable isotopes are used to more precisely infer plant physiological processes and environmental conditions. Studies have shown that isotopic ratios of

carbon and oxygen of tree ring cellulose ($\delta^{13}C_{cell}$, $\delta^{18}O_{cell}$) provide valuable information about plant C and water relations (Saurer *et al.,* 1997; Barnard *et al.,* 2012) and past environmental conditions (Roden *et al.,* 2000; Brooks & Mitchell, 2011). The $\delta^{13}C_{cell}$ reflects gas exchange by the plant at the time the C was fixed and can be used as a measure of intrinsic WUE defined as the ratio of A/g_s (Farquhar *et al*, 1989b) unless disproportionate changes in mesophyll conductance (g_m) have occurred (Flexas *et al.,* 2012).

However, it would also be useful to retrospectively separate the effects of variation in A and g_s on intrinsic WUE as indicated by $\delta^{13}C_{cell}$. The O isotope ratio of plant cellulose, $\delta^{18}O_{cell}$, has been shown to be useful for separating variation in A and g_s because the $\delta^{18}O_{cell}$ is only influenced by the water cycle, including g_s, and not A (Scheidegger *et al.,* 2000). Studies typically state that $\delta^{18}O_{cell}$ is influenced by the isotopic composition of source water, atmospheric water vapor, evaporative enrichment of leaf water (Roden *et al.,* 2000; Barbour, 2007) and a biochemical fractionation factor associated with incorporation of sugars into tree-ring cellulose (Yakir & DeNiro, 1990). Transpiration (E) from the leaf is controlled by the leaf-to-air vapor pressure deficit (VPD) and stomatal and boundary layer conductances. Therefore, in co-occurring trees that rely on identical sources of water and experience similar relative humidity (RH) and VPD, differences in $\delta^{18}O_{cell}$ should result from differences in g_s and therefore E. However, studies have found that the use of the dual isotope ($\delta^{13}C_{cell}$ and $\delta^{18}O_{cell}$) approach to compare treatment groups is complicated

even when environmental conditions such as source water, water vapor, RH, and T_{leaf} are the same among treatments (Brooks & Coulombe, 2009). Other factors besides *A* and g_s that are not accounted for by the dual isotope approach such as g_m and effective pathlength (*L*, the tortuosity of the pathway from the xylem to chloroplast and evaporative site) also influence gas exchange and thus $\delta^{13}C_{cell}$ and $\delta^{18}O_{cell}$ (Kahmen *et al*. 2008; Ferrio *et al*. 2012). These characteristics related to leaf anatomy may be influenced by the presence of dwarf mistletoe since it has been shown to alter water relations and hydraulic architecture (Meinzer *et al*. 2004), leaf size (Reblin *et al*., 2006), and leaf anatomy (Chhikara & Ross Friedman, 2008) of host trees.

Although tree-ring C and O stable isotopes have been used to investigate the effect of insects (Haavik *et al.*, 2007; Simard *et al.*, 2012) on host physiology, to our knowledge, the dual isotope approach has not been used to evaluate the effect of a parasitic plant on the physiology of its host. To improve our understanding of the integrated effects of hemlock dwarf mistletoe on host physiology over time, I compared annual radial growth, $\delta^{13}C_{cell}$, and $\delta^{18}O_{cell}$ of co-occurring uninfected and infected old-growth western hemlock trees in southwestern Washington to evaluate the utility of the dual isotope approach and the long-term effects of the infection on host photosynthetic gas exchange. I applied an established leaf water oxygen isotope fractionation model and previous physiological measurements to estimate g_m and *L* to detect potential infection-induced changes in leaf anatomy (Roden *et al.*, 2000; Barbour, 2007). Based on previous measurements of photosynthetic gas exchange and

leaf-specific hydraulic conductivity (Meinzer *et al.*, 2004), I expected infected trees to have reduced radial growth, lower $\delta^{13}C_c$, and similar $\delta^{18}O_{cell}$ to uninfected trees.

MATERIALS AND METHODS

Study species

Hemlock dwarf mistletoe (*A. tsugense*) infects western hemlock (*T. heterophylla*) along the west coast of North America from northern California to southeast Alaska and is found further north than any other dwarf mistletoe species (Hennon *et al.,* 2001). Hemlock dwarf mistletoes are dioecious and produce nectar-bearing flowers during mid-late summer. After pollination, fruits take 13-14 months to mature. Seeds are explosively discharged horizontally up to 15 m from a single-seeded berry, causing dwarf mistletoe populations to be clumped based on stand composition. Once attached to a branch, the seed establishes a holdfast structure to develop its endophytic system and haustorial connections with host phloem and xylem (Hawksworth & Wiens, 1996). Hemlock dwarf mistletoes induce localized branch infections visible as spindle-shaped swellings (Geils *et al.,* 2002). Diminutive aerial shoots erupt from these swellings approximately 2-7 years after seed germination (Geils *et al.,* 2002). Downstream from swellings, the host tree forms dense, fan-shaped branching systems called 'witches' brooms' that develop over a period of several years to decades.

Study area

The study site is located at the Wind River Field Station (WRFS) formerly the Wind River Canopy Crane Research Facility in the Wind River Experimental Forest, in southwest Washington State (45.820 lat, -121.952 lon) at an elevation of 368 m. Very wet winters and relatively dry summers characterize the climate. Average annual precipitation is 2176 mm with more than 90% falling during the rainy season of October-May (Carson Fish Hatchery, WA, Western Regional Climate Center). Average winter (December-March) and summer (June-September) temperatures are 2°C and 16°C, respectively. The stand is dominated by old-growth western hemlock (~250 years old; 224 ha^{-1}) and Douglas-fir (*Pseudotsuga menziesii*, ~450 years old; 35 ha^{-1}). It was originally populated with Douglas-fir, a pioneer species, from 1500 to 1600 AD while western hemlock, a secondary successional species, was reproducing in the understory. Stand density is about 427 trees ha^{-1}.

Monthly values of precipitation, mean air temperature (T_{air}), minimum air temperature (T_{min}), maximum air temperature (T_{max}), and dewpoint temperature were obtained from the PRISM Climate Group (Oregon State University, http://prism.oregonstate.edu). Relative humidity (RH) and VPD were estimated from T_{air} and dewpoint temperature using an algorithm for saturated vapor pressure (Paw U & Gao, 1988). Monthly Palmer Drought Severity Index (PDSI) values were obtained for nearby Climate Divisions for Oregon and Washington from the IRI/LDEO climate data library (http://iridl.ldeo.columbia.edu/). Growing season was considered to be May (day of year, DOY 121)-September (DOY 273). Daytime T_{air} and RH were estimated from equations ($y = 0.4715x + 10.892$; $y = 0.3191x + 40.715$, respectively)

relating annual PRISM climate variables to the mean monthly daytime (0630-1930h) values measured at the Wind River Canopy Crane Research Facility (University of Washington, http://depts.washington.edu/wrccrf/metdata/data/).

Assessment of dwarf mistletoe infection severity

All old-growth western hemlock trees at the site were surveyed for dwarf mistletoe infection severity using the Hawksworth 6-class dwarf mistletoe rating (DMR) system (Hawksworth & Wiens, 1996). Trees were inspected from the ground with binoculars. From observation, the crown is divided into thirds whereby each third is visually evaluated on a scale of 0-2; 0 is assigned to a third that displays 0% of branches infected, 1 for <50% infected, and 2 for >50% infected. The sum of the 0-2 evaluations for each third is the DMR classification. DMR 0 refers to uninfected trees and DMR 6 refers to heavily infected trees. Sampled heavily infected trees had significant signs of infection including formation of fan-shaped "witches' brooms", branch dieback, and broken treetops.

Sampling

Thirteen uninfected (DMR 0, uninfected group) and seventeen heavily infected (DMR 6, infected group) co-occurring western hemlock trees of approximately the same stem diameter (at 1.3m height), age, and tree height were sampled for growth and stable isotope analyses (Table 1). Stem diameter and age were measured for all selected trees; whereas height was recorded for a subset of 8 uninfected and 9 infected

trees. Stem diameter, height, and age were not significantly different between groups (Table 1). In July 2011, two 5-mm cores to pith and two 12-mm cores to approximately 10 cm depth at 180° from each other were extracted from each tree at approximately 1.3 m height. Cores were mounted, dried, and sanded. Ring widths were measured using a sliding stage incremental micrometer (Velmex Inc., Bloomfield, NY, USA) with Measure J2X software (VoorTech Consulting, Holderness, NH, USA). Visual cross-dating was verified using the COFECHA program to identify false or missing rings (Holmes, 1983) for all cores collected. To compare levels of tree growth, ring width data were converted to basal area increment (BAI, cm^2/year) assuming a circular outline of stem cross-sections. To account for tree size-related differences in growth during ontogeny, cross-dated BAI series were converted to relative basal area increment (RBAI) by dividing the BAI of a given year by the total basal area calculated for the same year. For comparing inter-annual variability in growth to climate variables, the cross-dated ring width series were detrended and standardized to produce ring width index chronologies using the program ARSTAN (Cook & Holmes, 1986). To create chronologies for each of the DMR 0 and DMR 6 groups, each ring-width series was detrended twice with either a linear or negative exponential regression in the first round to remove age-related trends. The second round of interactive detrending fit a flexible spline to each ring width index series to remove trends associated with canopy disturbances. These methods result in a more coherent inter-annual climate signal for shade-tolerant tree species such as western hemlocks that establish under closed canopy forest conditions

and are often exposed to highly dynamic resource availability after canopy gap-formation disturbances (Cook, 1985).

Sample preparation

Cores from a subset of 6 trees that had ring widths closest to the mean per group were processed for stable isotope analysis for two different objectives. The first objective was to obtain a long-term trend in $\delta^{13}C$ to potentially evaluate shifts in physiology associated with mistletoe infection. Five-year groupings of annual growth rings alternating every five years were separated from the 5 mm cores along the entire core length, spanning over 100 years. Growth and C isotope analyses from cores collected in 2002 from 3 uninfected and 2 infected trees from the same stand in the WRFS (DR Woodruff, unpublished data) supplemented cores collected in 2011 for a total sample size of 9 uninfected and 8 infected trees analyzed in growth and long-term C isotope campaigns. Analyses with and without the 2002 cores were not significantly different (data not shown).

The second objective was to evaluate more recent physiological differences between the two DMR classes using both isotopes. I used the shorter 12 mm cores, and selected two of the wettest and two of the driest years per decade spanning 1980-2010 for C and O isotope analyses based on precipitation and temperature data (PRISM Climate Group, Oregon State University). I expected dwarf mistletoe-induced shifts in stomatal behavior and gas exchange to be most pronounced during drier years because they would pose the most extreme evaporative demands (McCarroll &

Loader, 2004). The two wettest and two driest years that were selected per decade from 1980 to 2010 included: 1983, 1984, 1996, 1997, 2004, and 2010 and dry years were: 1987, 1989, 1992, 1999, 2006, and 2007. Each selected annual ring was separated with a razor blade and ground with a tissue homogenizer. All samples were extracted for alpha-cellulose. Oils and resins were removed with toluene-ethanol and ethanol Soxhlet extractions (Leavitt & Danzer, 1993). Holocellulose was isolated by delignification in an acetic acid-acidified sodium chlorite solution and converted to alpha-cellulose in sodium hydroxide (Sternberg, 1989).

Approximately 0.8 mg and 0.4 mg of alpha-cellulose was packed in tin and silver capsules for C combustion and O pyrolysis, respectively. C and O isotopic results are reported in per mil (‰, parts per thousand) and expressed in relation to the Vienna Peedee Belemnite (VPDB) or Vienna Standard Mean Ocean Water (VSMOW) standards, respectively. The isotope composition of C and O is represented by delta (δ) notation (expressed in parts per thousand, ‰) with reference to the standard material:

$$\delta^{13}C \quad or\ \delta^{18}O \quad = \left(\frac{R_{sample}}{R_{standard}} - 1\right) \qquad \text{Eqn 1}$$

$\delta^{13}C$ analyses of tree ring cellulose from five-year groupings were analyzed at Oregon State University's College of Earth, Oceanic, Atmospheric Sciences (CEOAS) stable isotope lab (OSU, Corvallis, OR). Samples were combusted to CO_2 in a Carlo Erba NA1500 elemental analyzer then introduced into a DeltaPlusXL isotope ratio mass spectrometer. IAEA-600 caffeine was used as a check standard and runs were calibrated daily using the international standards USGS40 glutamic acid and ANU

sucrose. Typical error was ± 0.1‰ or better as determined by repeated measures of internal quality control standards and from sample replicates.

$\delta^{13}C$ and $\delta^{18}O$ analyses of tree ring cellulose from the selected years were carried out at the University of California-Davis Stable Isotope Facility (UC-Davis, Davis, CA). Samples were analyzed for ^{13}C using a PDZ Europa ANCA-GSL elemental analyzer interfaced to a PDZ Europa 20-20 isotope ratio mass spectrometer (Sercon Ltd., Cheshire, UK). Samples were analyzed for ^{18}O using an elemental PyroCube (Elementar Analysensysteme GmbH, Hanau, Germany) interfaced to a PDZ Europa 20-20 isotope ratio mass spectrometer (Sercon Ltd., Cheshire, UK). Internal lab standards glutamic acid and alanine were used for order correction, size correction, and elemental amounts. IAEA-601 and IAEA-602 benzoic acid was used for scale normalization. Typical error was ± 0.2‰ or better as determined by repeated measures of internal quality control standards and from sample replicates.

Theory and Modeling

The $\delta^{13}C$ of whole leaf tissue ($\delta^{13}C_{leaf}$) incorporates the $\delta^{13}C$ of CO_2 in the atmosphere ($\delta^{13}C_{air}$), and fractionation against the heavy isotope which is influenced by the ratio of the concentration of CO_2 inside the leaf and thus the chloroplast (c_c, Seibt *et al.*, 2008) to that in the ambient air (c_a) described by the equation:

$$\delta^{13}C_{leaf} = \delta^{13}C_{air} - a - (b - a)\frac{c_c}{c_a} \qquad \text{Eqn 2}$$

where *a* is the fractionation effect associated with diffusion of CO_2 through stomata (4.4‰) and *b* is the fractionation effect (27‰) associated with discrimination against ^{13}C by the enzyme RUBISCO (ribulose bisphosphate carboxylase-oxygenase) during C fixation (Farquhar *et al.*, 1982; Farquhar *et al.*, 1989a). Values for $\delta^{13}C_{air}$ were obtained from the Scripps CO_2 Program (http://scrippsco2.ucsd.edu/). Values of $\delta^{13}C_{leaf}$ can be converted to $\Delta^{13}C$ to remove the impact of variation of $\delta^{13}C_{air}$ on $\delta^{13}C_{leaf}$ values over time (Brooks & Mitchell, 2011); however, in this study, uninfected and infected trees were sampled from the same stand and thus experienced the same environmental conditions (and same $\delta^{13}C_{air}$). Therefore, the differences in $\delta^{13}C_{leaf}$ between groups would not be significantly different from the differences in $\Delta^{13}C$ between groups. Eqn 2 describes products first formed by photosynthesis. However, the C isotope composition of cellulose ($\delta^{13}C_{cell}$) has a higher $\delta^{13}C$ value (2-5‰) than the first products of *A* due to other fractionation processes that occur during further metabolism (Leavitt & Long. 1982).

Values of $\delta^{13}C_{leaf}$ and thus $\delta^{13}C_{cell}$ reflect factors that regulate the amount of CO_2 fixed into photosynthate and tree ring cellulose. These factors include A_{max} (the biochemical capacity to fix C), and the conductance of CO_2 from the atmosphere to the sites of carboxylation which influences c_i and thus c_c. The conductance of CO_2 from the atmosphere to the sites of carboxylation in the chloroplast includes conductance of CO_2 from the atmosphere to intercellular spaces through stomata (g_s), as well as the conductance of CO_2 from the intercellular air spaces into the chloroplast

through the mesophyll (g_m). This pathway from atmosphere to intercellular spaces to chloroplast is complex, varies greatly between species, and can be influenced by leaf and cell membrane thickness, cell shape, and position of mesophyll cells and stomata (Evans *et al.*, 2009). Thus, $\delta^{13}C_{leaf}$ and thus $\delta^{13}C_{cell}$ reflects A_{max} and both g_s and g_m, despite the fact that many models neglect the influence of g_m because g_s and g_m are often assumed to be correlated (Flexas *et al.*, 2012). Nonetheless, $\delta^{13}C_{cell}$ can be used to estimate the relative stomatal and mesophyll limitation of *A* and intrinsic WUE (McCarroll & Loader, 2004).

A-c_i curves were measured on uninfected and infected western hemlock (n=3) from the same stand in 2002 (Meinzer *et al.*, 2004). *A*-c_i curves of uninfected and infected trees were described by the following equation:

$$A = y_0 + a(1 - e^{-bx}) \qquad \text{Eqn 3}$$

Equation parameters are included in Table 2. The initial slope of an *A*-c_i curve provides an estimate of g_m because g_m is a key determinant of *A* at low c_i (Lambers *et al.*, 2008). The initial slopes of the *A*-c_i curves for values of $c_i \leq 300$ ppm were used to estimate mesophyll conductance (g_m) in uninfected and infected trees.

The Craig-Gordon model describes the theoretical relationship between the variation in water $\delta^{18}O$ and RH and was first developed for evaporation from open bodies of water (Craig & Gordon, 1965). The model has been adapted to describe evaporative enrichment of leaf water (Farquhar & Lloyd, 1993) which incorporates differences in leaf temperature (T_{leaf}) and T_{air} through temperature effects on vapor

pressure. The Craig-Gordon model describes water enrichment under steady-state conditions at the site of evaporation:

$$\delta^{18}O_e = \delta^{18}O_s + \varepsilon* + \varepsilon_k + \left(\delta^{18}O_v - \delta^{18}O_s - \varepsilon_k\right)\frac{e_a}{e_i} \quad \text{Eqn 4}$$

where $\delta^{18}O_e$, $\delta^{18}O_s$, and $\delta^{18}O_v$ represent the O isotopic composition of leaf water at the site of evaporation, source water, and atmospheric water vapor, respectively, e_a/e_i is the ratio of ambient vapor pressure to saturation vapor pressure within the leaf (affected by T_{leaf}), ε* is the equilibrium fractionation between liquid water and vapor, and ε_k is the kinetic fractionation factor of vapor diffusion from the leaf to the atmosphere.

Leaf water isotopic heterogeneity can be explained further by the Péclet effect, which describes the ratio between the mass flow (advection) of unenriched source water to the evaporative sites through transpiration and the back diffusion of enriched water from the sites of evaporation (Farquhar & Lloyd, 1993; Barbour *et al*. 2000). The steady state isotopic enrichment of mean leaf lamina water ($\delta^{18}O_{lw}$) is described by Farquhar & Lloyd (1993):

$$\delta^{18}O_{lw} = \delta^{18}O_e \frac{(1-e^{-\wp})}{\wp} \quad \text{Eqn 5}$$

$$\wp = \frac{E\,L}{C\,D} \quad \text{Eqn 6}$$

where $\wp$ is the Péclet number describing the ratio of advection to diffusion, *E* is the leaf transpiration rate (mol m^{-2} s^{-1}), *L* is the scaled effective pathlength (m) for water movement from the veins to the site of evaporation, *C* is the molar density of water (55.56 10^3 mol m^{-3}), and *D* is the diffusivity of the heavy water isotopologue ($H_2{}^{18}O$)

in water (2.66 x 10^{-9} m^2s^{-1}). *L* is defined as the product of two components: *l*, the actual distance of the water pathway from xylem to the evaporative surface, and *k*, a scaling factor that accounts for the tortuosity of the path of water through a porous medium (Farquhar & Lloyd, 1993; Barbour & Farquhar, 2000; Cuntz *et al.*, 2007).

The incorporation of the $\delta^{18}O_{lw}$ signal into cellulose of plant tissue is described by the following equation (Barbour & Farquhar, 2000):

$$\delta^{18}O_{cell} = \delta^{18}O_{lw}\,(1 - p_{ex}p_x) + \varepsilon_o \qquad \text{Eqn 7}$$

where p_{ex} is the proportion of oxygen atoms that exchange with source water during cellulose formation, and p_x is the proportion of unenriched water (xylem water) at the site of cellulose formation, which for wood collected from the main trunk is equivalent to 1. ε_o is a fractionation factor of +27‰ associated with the water/carbonyl interactions (Yakir & DeNiro, 1990).

We used the Craig-Gordon model with the Péclet effect incorporated (termed Craig-Gordon Péclet model) to estimate *L* for uninfected and infected trees using tree ring $\delta^{18}O_{cell}$ from 1999, daytime RH, T_{air}, and T_{leaf} (where $T_{leaf} = T_{air} + 1.5^oC$), and g_s measured in 2002. The year 2002 (when *A*-c_i curves were collected) was not selected for C and O isotope analyses and 1999 was a year selected for C and O isotope analyses that was closest to 2002 with similar climate conditions (T_{air}, RH, VPD; Appendix A). *L* was adjusted until the model prediction of $\delta^{18}O_{cell}$ matched the observed $\delta^{18}O_{cell}$. Meinzer *et al*. (2004) measured g_s and *E* diurnally (4-6 sampling times/day, 0545 to 1640 h) on three branches of uninfected and infected western

hemlock trees (n=3) using a steady state porometer (LI-1600, LiCor Inc.) on four days during the 2002 growing season (17 July, 8 August, 28 August, 19 September or DOY 198, 220, 240, 262). I assumed the measured *E* of leaves enclosed in the ventilated porometer chamber reflected *E* of unenclosed leaves because the humidity balance point was set at the ambient value prior to each measurement and T_{leaf} in the chamber was close to T_{air}. Porometer measurements of g_s and *E* are therefore not independent because g_s is calculated based on *E*.

Statistical analyses

Simple linear regression was used to determine slope and intercept of RBAI, $\delta^{13}C_{cell}$, and $\delta^{18}O_{cell}$ vs. year; $\delta^{13}C_{cell}$ vs. $\delta^{18}O_{cell}$; and $\delta^{13}C_{cell}$, $\delta^{18}O_{cell}$, and ring width indices vs. climate variables. Extra sum of squares F-tests were used to determine if there was a significant interaction between group and year on RBAI, $\delta^{13}C_{cell}$, and $\delta^{18}O_{cell}$.To determine differences in RBAI, $\delta^{13}C_{cell}$, and $\delta^{18}O_{cell}$ between uninfected and infected trees, repeated measures analysis was used with a compound symmetry correlation structure with tree as a grouping factor (significance level was $P \leq 0.05$). The model of best fit was selected based on BIC (Bayesian information criterion) values. RBAI was log transformed to meet model assumptions of equal variance and normality. However, for ease of interpretation, I present back transformed data in results and figures. A two-sample t-test compared mean differences in tree diameter, height, age, $\delta^{13}C_{cell}$, $\delta^{18}O_{cell}$, *L*, g_m, and g_s between groups and $\delta^{13}C_{cell}$ and $\delta^{18}O_{cell}$ between wet and dry years. Statistical analyses were conducted in SigmaPlot 12.3

(Systat Software, San Jose, CA) and R version 2.15.2 (2012-10-26, The R Foundation for Statistical Computing). Error bars represent one standard error (SE).

RESULTS

For the period 1876-2010, there was a significant interaction between group and year on RBAI ($P = 0.0015$; Fig. 1a) but not on $\delta^{13}C_{cell}$ ($P = 0.083$; Fig. 1b). The intercept and rate of decline in RBAI in infected trees were significantly greater than those of uninfected trees ($P = 0.0025$, 0.0019, respectively, not shown). RBAI of infected trees was significantly greater than uninfected trees during 1886-1890, 1956-1960, and 1966-1970, while during 2006-2010, infected trees had lower RBAI than uninfected trees ($P \leq 0.05$, Fig. 1a).

Infected trees had significantly lower $\delta^{13}C_{cell}$ than uninfected trees during 1996-2000 and 2006-2010 ($P \leq 0.05$, Fig. 1b). Mean $\delta^{13}C_{cell}$ of infected trees displayed an asymptotic relationship with mean RBAI, whereby $\delta^{13}C_{cell}$ was reduced sharply at RBAI values below about 0.05 ($P < 0.0001$, $r^2 = 0.85$). This threshold level of RBAI was near the minimum RBAI displayed by non-infected trees. No significant linear nor curvilinear relationship was found between RBAI and $\delta^{13}C_{cell}$ of uninfected trees ($P = 0.46$, 0.16, respectively, Fig. 2). Contrary to expectations, correlations between ring widths and growing season climate variables were not significant for either group (Appendix B).

$\delta^{13}C_{cell}$ and $\delta^{18}O_{cell}$ were analyzed for selected wet and dry years for the period 1980-2010. There was no interaction between group and year on $\delta^{13}C_{cell}$ and $\delta^{18}O_{cell}$ of

selected years. Consistent with the long-term 5-year $\delta^{13}C_{cell}$ results (Fig. 1b), infected trees had significantly lower mean $\delta^{13}C_{cell}$ for the selected years during 1980-2010 ($P = 0.0001$, Fig. 3), where mean $\delta^{13}C_{cell}$ of uninfected trees was -24.1± 0.12‰ and infected trees was -25.4 ± 0.16‰. Contrary to expectations, infected trees had significantly lower $\delta^{18}O_{cell}$ than uninfected trees ($P = 0.003$, Fig. 3), despite that diurnal g_s (Appendix C) and E were not significantly different between uninfected and infected trees ($P = 0.36$). Mean $\delta^{18}O_{cell}$ of uninfected trees was 26.0 ± 0.5‰ and for infected trees it was 23.8 ± 0.2‰. Also contrary to expectations, wet and dry years had similar values for both $\delta^{13}C_{cell}$ and $\delta^{18}O_{cell}$ within uninfected and infected groups ($P = 0.94$, 0.20 (uninfected); 0.49, 0.75 (infected), respectively). Correlations between $\delta^{13}C_{cell}$ and $\delta^{18}O_{cell}$ with growing season climate variables (daytime T_{air}, RH, VPD, and precipitation) were not significant for either group (Appendix D).

There was a significant positive linear relationship between mean $\delta^{13}C_{cell}$ and $\delta^{18}O_{cell}$ across uninfected and infected trees ($P < 0.001$, $r^2 = 0.81$, Fig. 4) although within each group, the relationship was only significant for the uninfected trees (slope = 1.7, $P = 0.007$, $r^2 = 0.54$). For growth rings laid down in 1999, infected trees had significantly lower mean $\delta^{13}C_{cell}$, $\delta^{18}O_{cell}$, and g_m and significantly greater L than uninfected trees ($P \leq 0.05$, Table 3).

DISCUSSION

The integrated effects of long-term dwarf mistletoe infection on host western hemlock trees were recorded in the growth, $\delta^{13}C_{cell}$, and $\delta^{18}O_{cell}$ of tree rings. The

radial growth and $\delta^{13}C_{cell}$ trajectories described the intensification of dwarf mistletoe throughout host tree crowns. Heavily infected western hemlock trees had lower RBAI and $\delta^{13}C_{cell}$ than uninfected trees, consistent with previous studies that investigated the effects of dwarf mistletoe on host radial growth and physiology (Meinzer *et al.,* 2004; Stanton, 2007; Shaw *et al.,* 2008; Logan *et al.,* 2012). However, O isotope theory that attributes changes in $\delta^{18}O_{cell}$ to factors that influence the vapor pressure gradient from atmosphere to leaf, such as climate or g_s, and the dual isotope approach that is typically used to determine stomatal limitation of A_{max}, did not explain the lower $\delta^{18}O_{cell}$ values observed in heavily infected trees. Unlike previous studies that attributed changes in $\delta^{18}O_{cell}$ to variation in g_s or climate variables, $\delta^{18}O_{cell}$ was significantly different between uninfected and infected trees but could not be explained by variation in g_s or climate alone. Therefore, since dwarf mistletoe has been shown to impact host water relations and hydraulic architecture (Meinzer *et al.,* 2004), and leaf size and anatomy (Reblin *et al.,* 2006; Chhikara & Ross Friedman, 2008), I used the Craig-Gordon Péclet model and A-c_i curves to estimate L and g_m to determine if these leaf internal parameters could be driving the observed $\delta^{18}O_{cell}$ patterns since the $\delta^{18}O_{cell}$ differences between groups were not related to g_s or climate.

Growth and $\delta^{13}C_{cell}$

The combination of radial growth and $\delta^{13}C_{cell}$ analyses measured in tree rings of uninfected and infected trees described the intensification of dwarf mistletoe in the tree crowns and the progression of the infection through time. RBAI of trees that

became infected declined more rapidly than in trees that remained uninfected, suggesting that symptoms reported in previous studies—branch dieback and subsequent reduction in leaf area, photosynthetic tissue, *N* content in needles, and A_{max} (Meinzer *et al.*, 2004)—resulted in reduced radial growth as dwarf mistletoe intensified in the crown through time, proliferating throughout the host tree, and persisted as a nutrient sink (Flanagan *et al.,* 1993; Marshall *et al.,* 1994a, b; Cernusak *et al.,* 2004; Bickford *et al.,* 2005). RBAI of infected trees was significantly lower than uninfected trees in 2006-2010, consistent with other studies that observed reduced radial growth and stand basal area due to severe infection (Stanton, 2007; Shaw *et al.,* 2008; Logan *et al.,* 2012).

Tree diameter and RBAI calculated from ring widths suggested that infected trees were growing faster than uninfected trees prior to becoming infected (1886-1890, Fig. 1a). Consistent with this observation, Shaw *et al.* (2005) and Stanton (2007) hypothesized that larger, more vigorously growing trees are more likely to become infected. This may be due to more branch area available to intercept seed rain from animal vectors, the mechanism of dwarf mistletoe dispersal (Geils *et al.*, 2002). Larger trees may also be more likely to be infected because larger trees can survive with the infection longer than smaller trees. Sunlight is more available to taller trees rather than midstory trees and it has been shown that high light levels are required for aerial shoot production (Shaw & Weiss, 2000). Additionally, host *Pinus ponderosa* water and nutrient status has been shown to be positively correlated with dwarf mistletoe (*A.*

vaginatum subsp. *cryptopodum*) growth, suggesting that dwarf mistletoe robustness depends on host vigor (Bickford *et al.,* 2005).

The RBAI of infected trees was significantly greater in 1956-1960 and 1966-1970 than uninfected trees (Fig. 1a) which may have been associated with the formation of witches' brooms and the transient increase in host photosynthetic leaf area (Sala *et al.,* 2001) resulting in greater radial growth than that observed in uninfected trees. Witches' broom formations may be due to dwarf mistletoe-induced alterations in growth regulating hormones such as cytokinins. Logan *et al.,* (2012) found that host *Picea glauca* needles distal to dwarf mistletoe (*A. pusillum*) infections had 79% greater total cytokinin content than needles on uninfected branches. I hypothesize that hydraulic occlusion of host tree branches, swelling of branch spindles due to the physical obstruction by dwarf mistletoe sinkers and haustorium connections (Wilson & Calvin, 1996; Meinzer *et al.,* 2004), and interception of *N* by the parasite results in needle loss downstream from the localized infections. Needle shedding appeared to be a compensatory response to the dwarf mistletoe-induced hydraulic bottleneck (and lower branch hydraulic conductivity) to maintain leaf-specific conductivity (Meinzer *et al.*, 2004). Consequently, the remaining foliage with reduced A_{max} would not be able to support the respiratory demands of the increased branch area of witches' brooms. This would result in significant branch dieback observed in the field that contributes to significant reductions in radial growth observed in 2006-2010 when trees were severely infected. The radial growth trajectory based on tree ring

widths was a useful way to evaluate the intensification of dwarf mistletoe throughout host tree crowns over many decades.

Consistent with significantly lower radial growth in 2006-2010 in infected than uninfected trees, infected trees had significantly lower $\delta^{13}C_{cell}$ than uninfected trees during 1996-2000 and 2006-2010 (Fig. 1b). This result is consistent with significantly lower needle *N* content and A_{max} of infected relative to uninfected trees measured in 2002 in the same group of trees (Meinzer *et al.,* 2004) that influence $\delta^{13}C_{cell}$ and RBAI (Figs. 1a, 2). Leaves of trees infected with dwarf mistletoe have also been shown to have lower $\delta^{13}C$ values than those of uninfected trees (Sala *et al.,* 2001; Meinzer *et al.,* 2004, Logan *et al.,* 2012). The similar pattern found in tree ring cellulose and leaf cellulose shows that fractionation events that influence $\delta^{13}C$ at the leaf-level are reflected in $\delta^{13}C_{cell}$ of tree rings (Leavitt & Long, 1982). Infected trees displayed lower radial growth and $\delta^{13}C_{cell}$ concurrently relative to uninfected trees, supporting the hypothesis that heavily infected trees have lower A_{max} that contributes to reductions in radial growth as dwarf mistletoe intensifies in tree crowns. Interestingly, these patterns did not appear until 1996-2000 and 2006-2010 when trees were heavily infected, suggesting that the effects of dwarf mistletoe on the physiology of infected trees were not significant enough to be recorded in tree rings until trees became heavily infected. This is consistent with Shaw *et al.* (2008) that found that basal growth of lightly and moderately infected western hemlock trees at the Wind River site did not significantly differ from uninfected trees; however, severely infected trees grew from 16% to 46% less than uninfected trees. This further supports the hypothesis that there may be a

threshold at which infected trees become severely infected and exhibit the physiological impacts of the dwarf mistletoe infection.

This threshold in infected trees is described by the significant asymptotic relationship between RBAI and $\delta^{13}C_{cell}$ that was not present in uninfected trees (Fig. 2). As a function of how RBAI is calculated (BAI/basal area), in most individuals and species, RBAI declines as trees age and grow larger. Figure 2 shows that in uninfected trees, $\delta^{13}C_{cell}$ remained within similar ranges throughout the entire range of RBAI values. In contrast, in infected trees, $\delta^{13}C_{cell}$ was greater when RBAI was high but much lower when RBAI was low (Fig. 2). This describes the progression of the dwarf mistletoe intensification and its compound effects on host growth and A_{max}. As dwarf mistletoe proliferates throughout the host tree, N is diverted from the host tree, reducing host A_{max} and resulting in lower RBAI and lower $\delta^{13}C_{cell}$.The combination of radial growth and $\delta^{13}C_{cell}$ was a useful tool for tracking the progression and intensification of the dwarf mistletoe infection through time, in particular the threshold at which infected trees display significant physiological impacts of the infection. Because infected trees displayed effects of the infection only when trees were mostly heavily infected, radial growth and $\delta^{13}C_{cell}$ could not be used to identify exactly when trees were infected. However, based on the radial growth trajectories, I estimate that infected trees were infected approximately 1926-1930 and 1936-1940, several decades before witches' brooms presumably appeared. This allows for the incubation and latency periods of the dwarf mistletoe life cycle, as well as the development of

disruptions in growth regulating hormones that result in the formation of witches' brooms.

$\delta^{18}O_{cell}$

According to theory and previous work, variation in $\delta^{18}O_{cell}$ can be explained by environmental conditions (e.g. source water, RH) and tree physiological and leaf structural characteristics (e.g. L, g_m). Using the dual isotope approach (Scheidegger *et al.*, 2000) under similar environmental conditions across treatment groups, patterns in $\delta^{18}O_{cell}$ are interpreted as changes in g_s because g_s regulates E, evaporative enrichment of leaf water, and thus $\delta^{18}O_{cell}$. Therefore, I had hypothesized that $\delta^{18}O_{cell}$ of infected trees would not differ from that of uninfected trees because observed g_s of these co-occurring trees was not significantly different (Appendix C). However, I observed that infected trees had significantly lower $\delta^{18}O_{cell}$ than uninfected trees (Fig. 3) regardless of climate (Appendix D), suggesting that leaf structural characteristics rather than g_s, climate, or differences in how trees responded to climate, were driving the observed patterns in $\delta^{18}O_{cell}$.

Many studies using the dual isotope ($\delta^{13}C_{cell}$ and $\delta^{18}O_{cell}$) approach attributed changes in $\delta^{18}O_{cell}$ to tree responses to climate such as RH and VPD (Saurer *et al* 1997; Scheidegger *et al.*, 2000; Barbour *et al.*, 2002), thinning and fertilization that caused crown microclimate changes (Brooks & Mitchell, 2011), and seasonal changes in precipitation (Roden & Ehleringer, 2007). However, I ruled out differences in source water and microclimate conditions such as RH, VPD, and T_{air} as major drivers

behind the group differences in $\delta^{18}O_{cell}$ because uninfected and infected trees were sampled from the same stand and experiencing the same environmental conditions over time. Furthermore, the differences between DMR groups were consistent regardless of the annual climate. Study trees were also the same age and size at the time of the study (Table 1) and were infected decades after root systems were developed. Therefore, it is unlikely that uninfected and infected trees were accessing water at different depths (Brooks *et al.*, 2006), a factor known to influence $\delta^{18}O_{cell}$. In addition, ring width indices, $\delta^{13}C_{cell}$, and $\delta^{18}O_{cell}$ were not significantly correlated with climate variables for either group (Appendices B, D). The lack of correlation was likely due to the fact that g_s peaked when RH was high and VPD and T_{air} were low in the morning (Appendix C). This result implies that the majority of C eventually incorporated into tree ring cellulose was fixed into sugars prior to substantial diurnal decreases in RH and increases in VPD and T_{air}. At high RH, ^{18}O enrichment is relatively insensitive to large variation in g_s because evaporative demand is low. Therefore, even if large differences in g_s were measured between groups or between wet and dry years, they would be muted and difficult to detect.

Studies attribute a positive relationship between $\delta^{13}C_{cell}$ and $\delta^{18}O_{cell}$ to the response of g_s to shifts in A_{max} and environmental conditions such as RH, VPD, and soil moisture (Saurer *et al.*, 1997; Barbour *et al.*, 2002; Barnard *et al.*, 2012). Different slopes of the $\delta^{13}C_{cell}$ and $\delta^{18}O_{cell}$ relationship are often attributed to differences in stomatal responses to soil moisture and evaporative demand where higher isotope ratios and steeper slopes of the $\delta^{13}C_{cell}$ and $\delta^{18}O_{cell}$ relationship are found at drier sites

(Saurer *et al.,* 1997). However, the difference in slopes of the $\delta^{13}C_{cell}$ and $\delta^{18}O_{cell}$ relationship between uninfected and infected trees is not due to environmental conditions because trees were sampled from the same site and correlations between $\delta^{13}C_{cell}$ and $\delta^{18}O_{cell}$ and climate variables were low or not significant (Appendix D). The lack of relationship between $\delta^{13}C_{cell}$ and $\delta^{18}O_{cell}$ in infected trees suggests that changes in g_s did not substantially influence the C isotope composition of the tree ring cellulose (Fig. 4; Saurer *et al.,* 1997; Barbour *et al.,* 2002; Simard *et al.,* 2012). Therefore, reduced A_{max} appeared to be the primary driver behind patterns in $\delta^{13}C_{cell}$ consistent with field measurements of g_s (Appendix C) and the interpretation that infected trees lack stomatal adjustment in response to reductions in A_{max} (Meinzer *et al.,* 2004). Fig. 4 demonstrates how interpretations of the relative contributions of variation in A and g_s to variation in intrinsic WUE based on mean $\delta^{13}C_{cell}$ and $\delta^{18}O_{cell}$ can be misleading because the regression line through both groups suggested that $\delta^{13}C_{cell}$ and $\delta^{18}O_{cell}$ of infected trees were also significantly and positively related. However, the lack of relationship within the infected group enabled us to better tease apart differences between groups.

After ruling out climate and g_s as primary drivers behind the significant difference in $\delta^{18}O_{cell}$ between uninfected and infected trees, I considered leaf characteristics including g_m and L. Of the few studies quantifying the effects of dwarf mistletoe on host leaf anatomy, Chhikara & Ross Friedman (2008) found that vascular bundles of *Pinus contorta* needles downstream of dwarf mistletoe infections were positioned significantly closer together than in needles of uninfected trees, although

these results are limited to hosts with similar leaf anatomy as *P. contorta* (e.g. species with two vascular bundles). Previous work has shown that g_m is positively correlated with A_{max} under non-saturating CO_2 concentrations (Flexas *et al.,* 2008), consistent with lower A_{max} (Meinzer *et al.,* 2004) and lower g_m observed in infected trees (Table 3). In this study, lower A_{max} was likely caused by the diversion of *N* by the dwarf mistletoe infection while lower g_m was likely due to shifts in leaf anatomy and the diffusion path of CO_2 also induced by the infection. While studies show that the type of diffusing molecule, diffusion media, diffusion path, and environmental conditions influence g_m, the effective diffusion path distance is considered the chief determinant of g_m (Flexas *et al.,* 2012). Hydraulic conductance of the mesophyll is impossible to measure directly although whole leaf hydraulic conductance (K_{leaf}) is positively related to g_m which is likely due to anatomical limitations such as path distance to CO_2 and water conductances (Flexas *et al.,* 2012). Similarly, *L* describes the pathway of water movement from xylem to evaporative sites which influences $\delta^{18}O_{cell}$. Because the transport pathways for CO_2, water vapor, and liquid water overlap, it is not surprising that *L* and g_m are inversely related (Ferrio *et al.,* 2012): *L* accounts for both length of the pathway and its tortuosity. This inverse relationship is consistent with our findings that infected trees had lower g_m and greater *L* than uninfected trees (Table 3). However, it is difficult to quantify the relative contributions of each to variation in $\delta^{18}O_{cell}$ because g_m and *L* are influenced by similar leaf anatomical characteristics. Infected trees were estimated to have values of *L* roughly three times greater than

uninfected trees and values of g_m that were about 34% lower than uninfected trees (Table 3).

Values of *L* of uninfected and infected trees were consistent with those estimated in conifers in Song *et al*. (2013) that ranged from 0.05-0.4 m. The estimate of greater *L* in infected trees is consistent with higher values of $\wp$ and less back diffusion of enriched water from evaporative sites to the sites of carbohydrate synthesis in the leaf, ultimately resulting in lower values of $\delta^{18}O_{cell}$ in tree rings (Eqns 5, 6). Previous work employing the Craig-Gordon Péclet model showed that *L* was highly correlated with $\delta^{18}O_{lw}$ and that the effect of environmental parameters (RH, T_{air}) on $\delta^{18}O_{lw}$ was highly dependent on *L* (Kahmen *et al.,* 2008; Ferrio *et al.,* 2012; Song *et al.,* 2013). With increasing *L*, the Péclet effect became a more important determinant of ^{18}O enrichment in leaf water while environmental drivers, direct influences of g_s and *E,* became less important.

A sensitivity analysis comparing g_s and $\delta^{18}O_{cell}$ revealed that g_s would need to change by 84.0, 42.5, and 28.6 mmol m^{-2} s^{-1} to result in the observed 2.5‰ difference in $\delta^{18}O_{cell}$ (observed in 1999) at the values of *L* of 0.118 m (average uninfected L), 0.236 m (average uninfected and infected L), and 0.354 m (average infected L), respectively (Appendix E). Measured g_s in the field on four days throughout the 2002 growing season was not significantly different between groups (Appendix C); however, tree rings integrate over annual time scales. Therefore, four days of g_s measurements may not necessarily capture the same variation recorded in tree ring cellulose. Nonetheless, the sensitivity analysis provided evidence that even if

variations in g_s (not measured in the field) may have influenced tree ring $\delta^{18}O_{cell}$, g_s would need to be substantially different between groups to be the primary driver behind the 2.5‰ difference in $\delta^{18}O_{cell}$. Therefore, leaf characteristics related to *L*, rather than g_s, are likely driving the observed $\delta^{18}O_{cell}$ patterns.

Song *et al*. (2013) suggested that small decreases in *E* result in substantial increases in *L* at low *E* values (less than 1.50 mmol m^{-2} s^{-1}), typical of coniferous species (see Fig. 4 in Song *et al.*, 2013). This suggests that species that operate at low *E* can have substantially different *L* but similar *E*. Our findings that *E* of infected trees did not differ from uninfected trees, yet *L* was three times greater than uninfected trees, further suggested that differences in *L* were a stronger driver of variation in $\delta^{18}O_{cell}$ than variation in *E* in uninfected and infected western hemlock.

Mesophyll conductance is often ignored in gas exchange measurements and C isotope models although in some cases this may not be justified because g_m can change with environmental conditions and often more rapidly than g_s (Warren, 2007; Flexas *et al.*, 2008; Flexas *et al.*, 2012). For example, $\delta^{13}C_{cell}$ is a useful proxy to estimate relative stomatal limitation of *A* and intrinsic WUE (A/g_s; McCarroll & Loader, 2004) but may not be an accurate indicator of WUE where g_s and g_m are not strongly correlated (Lambers *et al*.; 2008; Seibt *et al.*, 2008). Shifts in g_m can lead to changes in c_c/c_a (vs c_i/c_a) that are not directly included in Eqn 2 (Farquhar *et al.*, 1982). This variation can be large enough to account for variations in $\delta^{13}C_{leaf}$ and thus $\delta^{13}C_{cell}$ (Seibt *et al.*, 2008). Although g_m was responsible for reductions in overall conductance to CO_2 (because g_s was similar between groups) in this study, the

infection-induced reduction in A_{max} was still the primary driver behind group differences in $\delta^{13}C_{cell}$ because infected trees had lower $\delta^{13}C_{cell}$, implying that ^{13}C discrimination and c_c/c_a were greater and A/g_s was significantly lower in infected than uninfected trees.

Nonetheless g_m and its relative contribution to the limitation of A_{max} and its co-regulation with g_s must be considered when interpreting $\delta^{13}C_{cell}$ and WUE, often used to predict how trees may respond to future shifts in climate (Sanguesa-Barreda *et al.,* 2012). However, it is difficult to incorporate g_m into photosynthesis and leaf water O isotope models due to the lack of sufficient knowledge about the mechanisms involved in regulation of g_m (Flexas *et al.,* 2012). Because I ruled out the influence of g_s and environmental variables on $\delta^{18}O_{cell}$, our results provide evidence that L and g_m were likely primary drivers behind the observed $\delta^{18}O_{cell}$ patterns. Additional investigations of the relationship between L and g_m may improve interpretations of $\delta^{13}C_{cell}$ and $\delta^{18}O_{cell}$. Future studies should investigate the effect of the dwarf mistletoe infection on leaf anatomical characteristics that influence g_m and L such as mesophyll cell wall thickness (Terashima *et al.,* 2006; Lambers *et al.,* 2008).

In conclusion, this study showed that the combination of radial growth and $\delta^{13}C_{cell}$ was a useful tool for tracking the progression and intensification of the dwarf mistletoe infection through time, in particular the threshold at which infected trees displayed significant physiological impacts of the infection. Because infected trees displayed impacts of the infection only when trees were mostly heavily infected, radial growth and $\delta^{13}C_{cell}$ could not be used to identify exactly when trees were infected.

However, radial growth trajectories described the progression of the infection by indicating that infected trees were larger than uninfected trees in the past, the formation of witches' brooms, and the eventual decline in growth as the infection intensified. The significant differences in L and g_m between uninfected and infected trees suggested that dwarf mistletoe may influence host leaf structure and anatomy characteristics that are related to these parameters. This study also points to the limitations of the dual isotope approach for identifying sources of variation in c_i/c_a and c_c/c_a and therefore $\delta^{13}C_{cell}$ (Roden & Farquhar, 2012) because it does not account for the physiological effects of pathogens nor leaf anatomical characteristics that affect L and g_m, which in turn influence $\delta^{18}O_{lw}$ and ultimately $\delta^{18}O_{cell}$. This study's results were consistent with those of recent studies that emphasize the importance of incorporating leaf anatomy, L, and g_m into interpretations of $\delta^{13}C_{cell}$ and $\delta^{18}O_{cell}$. These findings have important implications for reconstructing tree responses to climate fluctuations because undetected dwarf mistletoe or other pathogens that modify leaf anatomy and functioning may imprint an unknown degree of variability on stable isotope signatures presumed to be driven by climatic variation. Studies integrating leaf to whole-tree physiology will improve our understanding of the western hemlock-dwarf mistletoe system from the tree to canopy scale and better inform forest management decisions, especially since dwarf mistletoe has ecosystem-scale effects that are still being explored (Watson, 2001; Shaw *et al.*, 2004; Bell & Adams, 2011; Way, 2012).

ACKNOWLEDGEMENTS

I would like to thank Brandy Saffell for her help with field and lab work. This work was supported by the National Science Foundation under award number DEB-0743882.

REFERENCES

Barbour, MM, Walcroft AS, Farquhar, GD. 2002. Seasonal variation in $\delta^{13}C$ and $\delta^{18}O$ of cellulose from growth rings of *Pinus radiata*. *Plant, Cell & Environment* **25**: 1483–1499.

Barbour MM, Farquhar GD. **2000**. Relative humidity- and ABA-induced variation in carbon and oxygen isotope ratios of cotton leaves. *Plant, Cell & Environment* **23**: 473–485.

Barbour MM. 2007. Stable oxygen isotope composition of plant tissue: a review. *Functional Plant Biology* **34**: 83–94.

Barnard HR, Brooks JR, Bond BJ. 2012. Applying the dual-isotope conceptual model to interpret physiological trends under uncontrolled conditions. *Tree Physiology* **32**: 1183-1198.

Bell TL, Adams MA. 2011. Attack on all fronts: functional relationships between aerial and root parasitic plants and their woody hosts and consequences for ecosystems. *Tree Physiology* **31**:3-15.

Bickford CP, Kolb TE, Geils BW. 2005. Host physiological condition regulates parasitic plant performance: *Arceuthobium vaginatum* subsp. *cryptopodum* on *Pinus ponderosa*. *Oecologia* **146**: 179–189.

Brooks JR, Meinzer FC, Warren JM, Domec JC, Coulombe R. 2006. Hydraulic redistribution in a Douglas-fir forest: lessons from system manipulations. *Plant, Cell & Environment* **29**: 138-150.

Brooks JR, Coulombe R. 2009. Physiological responses to fertilization recorded in tree rings: isotopic lessons from a long-term fertilization trial. *Ecological Applications* 19: 1044-1060.

Brooks JR, Mitchell AK. 2011. Interpreting tree responses to thinning and fertilization using tree-ring stable isotopes. *New Phytologist* 190: 770-782.

Cernusak, Lucas A., John S. Pate, and Graham D. Farquhar. 2004. Oxygen and carbon isotope composition of parasitic plants and their hosts in southwestern Australia. *Oecologia* 139: 199-213.

Chhikara A, Ross Friedman CM. 2008. The effects of male and female *Arceuthobium americanum* (lodgepole pine dwarf mistletoe) infection on the relative positioning of vascular bundles, starch distribution, and starch content in *Pinus*

contorta var. *latifolia* (lodgepole pine) needles. *Botany* 86:539-543.

Cook ER. 1985. A time series approach to tree-ring standardization. Tucson, AZ: University of Arizona. 171 pp. Ph.D. dissertation.

Cook ER, Holmes RL. 1986. Users Manual for Program ARSTAN. Laboratory of Tree-Ring Research, University of Arizona, Tucson, USA.

Craig H, Gordon LI. 1965. Deuterium and oxygen-18 variation in the ocean and the marine atmosphere. In: Tongiorgi E, ed. Proceedings of a conference on stable isotopes in oceanographic studies and paleotemperatures. Spoleto, Italy: 9–130.

Cuntz M, Ogee J, Farquhar GD, Peylin P and Cernusak LA. 2007. Modelling advection and diffusion of water isotopologues in leaves. *Plant, Cell & Environment* 30: 892–909.

Evans JR, Kaldenhoff R, Genty B, Terashima I. 2009. Resistances along the CO2 diffusion pathway inside leaves. *Journal of Experimental Botany* 60: 2235-2248.

Farquhar GD, O'Leary MH, Berry JA. 1982. On the relationship between carbon isotope discrimination and the intercellular carbon dioxide concentration in leaves. *Australian Journal of Plant Physiology* 9:121-137.

Farquhar GD, Ehleringer JR, Hubick KT. 1989a. Carbon isotope discrimination and photosynthesis. *Annual Review of Plant Physiology and Molecular Biology* 40: 503–537.

Farquhar GD, Hubick KT, Condon AG, Richards RA. 1989b. Carbon isotope fractionation and plant water-use efficiency. In: Rundel PW, Ehleringer JR, Nagy KA, eds. Stable isotopes in ecological research. Berlin: Springer-Verlag, 21–40.

Farquhar GD, Lloyd J. 1993. Carbon and oxygen isotope effects in the exchange of carbon dioxide between terrestrial plants and the atmosphere. In: Ehleringer JR, Hall AE, Farquhar GD, eds. Stable isotopes and plant carbon-water relations. San Diego: Academic Press, 47–70.

Ferrio JP, Pou A Florez-Sarasa I, Gessler A, Kodama N, Flexas J, Ribas-Carbo M. 2012. The Péclet effect on leaf water enrichment correlates with leaf hydraulic conductance and mesophyll conductance for CO2. *Plant, Cell & Environment* 35: 611-625.

Flanagan LB, Marshall JD, Ehleringer JR. 1993. Photosynthetic gas exchange and the stable isotope composition of leaf water: comparison of a xylem-tapping mistletoe and its host. *Plant, Cell & Environment* 16: 623-631.

Flexas J, Ribas-Carbo M, Diaz-Espejo, A, Galmes J, Medrano H. 2008. Mesophyll conductance to CO2: current knowledge and future prospects. *Plant, Cell & Environment 31*: 602-621.

Flexas J, Barbour MM, Brendel O, Cabrera HM, Carriquí M, Diaz-Espejo A, Douthe C, Dreyer E, Ferrio JP, Gago J, Galle A, Galmes J, Kodama N, Medano H, Niinemets U, Pequero-Pina JJ, Pou A, Ribas-Carbo M, Tomas M, Tosens T, Warren CR. 2012. Mesophyll diffusion conductance to CO2: An unappreciated central player in photosynthesis. *Plant Science* 196: 70-84.

Geils BW, Tovar JC, Moody B. **2002**. Mistletoes of North American Conifers. General Technical Report RMRS-GTR-98.

Haavik LJ, Stephen FM, Fierke MK, Salisbury VB, Leavitt SW, Billings SA. 2007. Dendrochronological parameters of norther red oak infested with red oak borer. *Forest Ecology and Management* 255:1501-1509.

Hawksworth, FG, Wiens D. 1996. Dwarf mistletoes: Biology, pathology and systematics. Agriculture Handbook 709. Washington, DC: USDA Forest Service, 410 pp.

Hennon PE, Beatty JS, Hildebrand D. 2001. Western Hemlock Dwarf Mistletoe. Forest Insect & Disease Leaflet 135, USDA Forest Service.

Holmes RL. 1983. Computer-assisted quality control in tree-ring dating and measurement. *Tree-Ring Bulletin* 43: 69-78.

Hubbard RM, Ryan MG, Stiller V, Sperry JS. 2001. Stomatal conductance and photosynthesis vary linearly with plant hydraulic conductance in ponderosa pine. *Plant, Cell & Environment* 24: 113-121.

Hull RJ, Leonard OA. 1964. Physiological aspects of parasitism in mistletoes (Arceuthobium and Phoradendron). I. The carbohydrate nutrition of mistletoe. *Plant Physiology* 39: 996-1007.

Kahmen A, Simonin K, Tu KP, Merchant A, Callister A, Siegwolf R, Dawson TE, Arndt SK. 2008. Effects of environmental parameters, leaf physiological properties and leaf water relations on leaf water $\delta^{18}O$ enrichment in different Eucalyptus species. *Plant, cell & environment* 31: 738-751.

Lambers H, Chapin FS III, Pons TL. 2008. Plant physiological ecology. New York, US: Springer.

Leavitt SW, Long A. 1982. Evidence for 13C/12C fractionation between tree leaves and wood. *Nature* 298: 742-744.

Leavitt SW, Danzer SR. 1993. Methods for batch processing small wood samples to holocellulose for stable-carbon isotope analysis. Analytical Chemistry 65: 87–89.

Logan BA, Huhn ER, Tissue DT. 2002. Photosynthetic characteristics of eastern dwarf mistletoe (*Arceuthobium pusillum* Peck) and its effects on the needles of host white spruce (*Picea glauca* [Moench] Voss). *Plant Biology* 4: 740-745.

Logan BA, Reblin JS, Zonana DS, Dunlavey RF, Hricko CR, Hall AW, Schmiege SC, Buschek RA, Duran KL, Neil Emery RJ, Kurepin LV, Lewis JD, Pharis RP, Phillips NH, Tissue DT. 2012. Impact of eastern dwarf mistletoe (*Arceuthobium pusillum*) on host white spruce (*Picea glauca*) development, growth and performance across multiple scales. *Physiologia Plantarum* 147: 502–513.

Marshall JD, Dawson TE, Ehleringer JR. 1994a. Integrated nitrogen, carbon, and water relations of a xylem-tapping mistletoe following nitrogen fertilization of the host. *Oecologia* 100: 430-438.

Marshall JD, Ehleringer JR, Schulze ED, Farquhar G. 1994b. Carbon isotope composition, gas exchange and heterotrophy in Australian mistletoes. *Functional Ecology* 8: 237-241.

McCarroll D, Loader NJ. 2004. Stable isotopes in tree rings. *Quarternary Science Reviews* 23:771-801.

Meinzer FC, Woodruff DR, Shaw DC. 2004. Integrated responses of hydraulic architecture, water and carbon relations of western hemlock to dwarf mistletoe infection. *Plant, Cell and Environment* 27:937-946.

Paw U KT, Gao W. 1988. Applications of solutions to non-linear energy budget equations. *Agricultural and Forest Meteorology* 43: 121-145.

Reblin JS, Logan BA, Tissue DT. 2005. Impact of eastern dwarf mistletoe (*Arceuthobium pusillum*) infection on the needles of red spruce (*Picea rubens*) and white spruce (*Picea glauca*): oxygen exchange, morphology and composition. *Tree Physiology* 26: 1325-1332.

Roden JS, Ehleringer JR. 2007. Summer precipitation influences the stable oxygen and carbon isotopic composition of tree-ring cellulose in Pinus ponderosa. *Tree physiology* 27: 491-501.

Roden JS, Lin G, Ehleringer JR. 2000. A mechanistic model for interpretation of hydrogen and oxygen isotope ratios in tree-ring cellulose. *Geochimica et Cosmochimica Acta* 64: 21–35.

Roden JS, Farquhar GD. 2012. A controlled test of the dual-isotope approach for the interpretation of stable carbon and oxygen isotope ratio variation in tree rings. *Tree Physiology* 4: 490-503.

Sala A, Carey EV, Callaway RM. 2001. Dwarf mistletoe affects whole-tree water relations of Douglas fir and western larch primarily through changes in leaf to sapwood ratios. *Oecologia* 126: 42-52.

Sangüesa-Barreda G, Linares JC, Camarero JJ. 2013. Drought and mistletoe reduce growth and water-use efficiency of Scots pine. *Forest Ecology and Management* 296: 64-73.

Santiago LS, Goldstein G, Meinzer FC, Fisher JB, Machado K, Woodruff D, Jones T. 2004. Leaf photosynthetic traits scale with hydraulic conductivity and wood density in Panamanian forest canopy trees. *Oecologia* 140: 543-550.

Saurer M, Aellen K, Siegwolf R. 1997. Correlating δ13C and δ18O in cellulose of trees. *Plant, Cell & Environment* 20: 1543-1550.

Scheidegger Y, Saurer M, Bahn M, Siegwolf R. 2000. Linking stable oxygen and carbon stable isotopes with stomatal conductance and photosynthetic capacity: a conceptual model. *Oecologia* 125: 350-357.

Seibt U, Rajabi A, Griffiths H, Berry JA. 2008. Carbon isotopes and water use efficiency: sense and sensitivity. *Oecologia* 155: 441–454.

Shaw DC, Weiss SB. 2000. Canopy light and the distribution of hemlock dwarf mistletoe aerial shoots in an old-growth Douglas-fir/western hemlock forest. *Northwest Science*. 74: 306-315.

Shaw DC, Watson DM, Mathiasen RL. 2004. Comparison of dwarf mistletoes (*Arceuthobium spp., Viscaceae*) in the western United States with mistletoes (*Amyema spp., Loranthaceae*) in Australia--ecological analogs and reciprocal models for ecosystem management. *Australian Journal of Botany* 52:481-498.

Shaw DC, Chen J, Freeman EA, Braun DM. 2005. Spatial and population characteristics of dwarf mistletoe infected tree sin an old-growth Douglas-fir – western hemlock forest. *Canadian Journal of Forest Research* 35: 990-1001.

Shaw DC, Huso M, Bruner H. 2008. Basal area growth impacts of dwarf mistletoe on western hemlock in an old-growth forest. *Can. J. For. Res.* 38: 576-583.

Simard S, Morin H, Krause C, Buhay WM, Treydte K. 2012. Tree-ring widths and isotopes of artificially defoliated balsam firs: A simulation of spruce budworm outbreaks in Eastern Canada. *Environmental and Experimental Botany* 81: 44-54.

Song X, Barbour MM, Farquhar GD, Vann DR, Helliker BR. 2013. Transpiration rate relates to within- and across- species variations in effective pathlength in a leaf water model of oxygen isotope enrichment. *Plant, Cell & Environment*. doi: 10.1111/pce.12063.

Stanton S. 2007. Effects of dwarf mistletoe on climate response of mature ponderosa pine trees. *Tree-Ring Research* 63: 69-80.

Sternberg L. 1989. Oxygen and hydrogen isotope measurements in plant cellulose analysis. Pages 89-99 *in* H. F. Linskens and J. F. Jackson, editors. Modern Methods of Plant Analysis Vol 10: Plant Fibers. Springer Verlag, Berlin.

Terashima I, Hanba YT, Tazoe Y, Vyas P, Yano S. 2006. Irradiance and phenotype: comparative eco-development of sun and shade leaves in relation to photosynthetic CO2 diffusion. *Journal of Experimental Botany* 57: 343–354.

Warren CR, Löw M, Matyssek R, Tausz M. 2007. Internal conductance to CO2 transfer of adult *Fagus sylvatica*: Variation between sun and shade leaves and due to free-air ozone fumigation. *Environmental and Experimental Botany* 59: 130-138.

Watson DM. 2001. Mistletoe--A Keystone Resource in Forests and Woodlands Worldwide. *Annual Review of Ecology and Systematics* 32:219-249.

Way D. 2011. Parasitic plants and forests: a climate change perspective. *Tree Physiology* 31:1-2.

Wilson CA, Calvin CL. 1996. Anatomy of the dwarf mistletoe shoot system, pp. 95–111. *In* F. G. Hawksworth and D. Wiens [eds.], *Dwarf Mistletoes: Biology, Pathology, and Systematics*. USDA, FS, Washington, D.C.

Yakir D, DeNiro MJ. 1990. Oxygen and hydrogen isotope fractionation during cellulose metabolism in *Lemna gibba* L. *Plant Physiology* 93: 325–332

Zweifel R, Bangerter S, Rigling A, Sterck FJ. 2012. Pine and mistletoes: how to live with a leak in the water flow and storage system? *Journal of Experimental Botany* 63: 2565-2578.

FIGURES

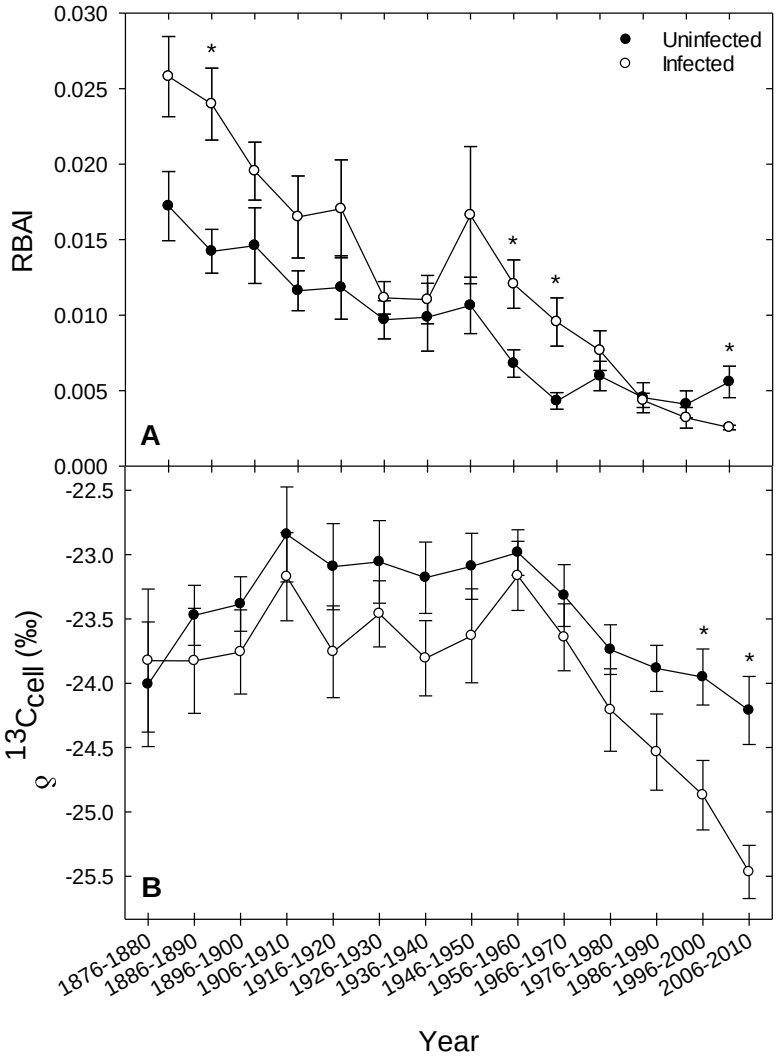

Figure 1. Mean ± SE of (**A**) 5-year RBAI and (**B**) 5-year $\delta^{13}C_{cell}$ of uninfected (closed circles, n=9) and infected (open circles, n=8) trees for the period 1876-1880 to 2006-2010. Asterisks represent significant differences in repeated measures ANOVA ($P \leq 0.05$) between uninfected and infected trees.

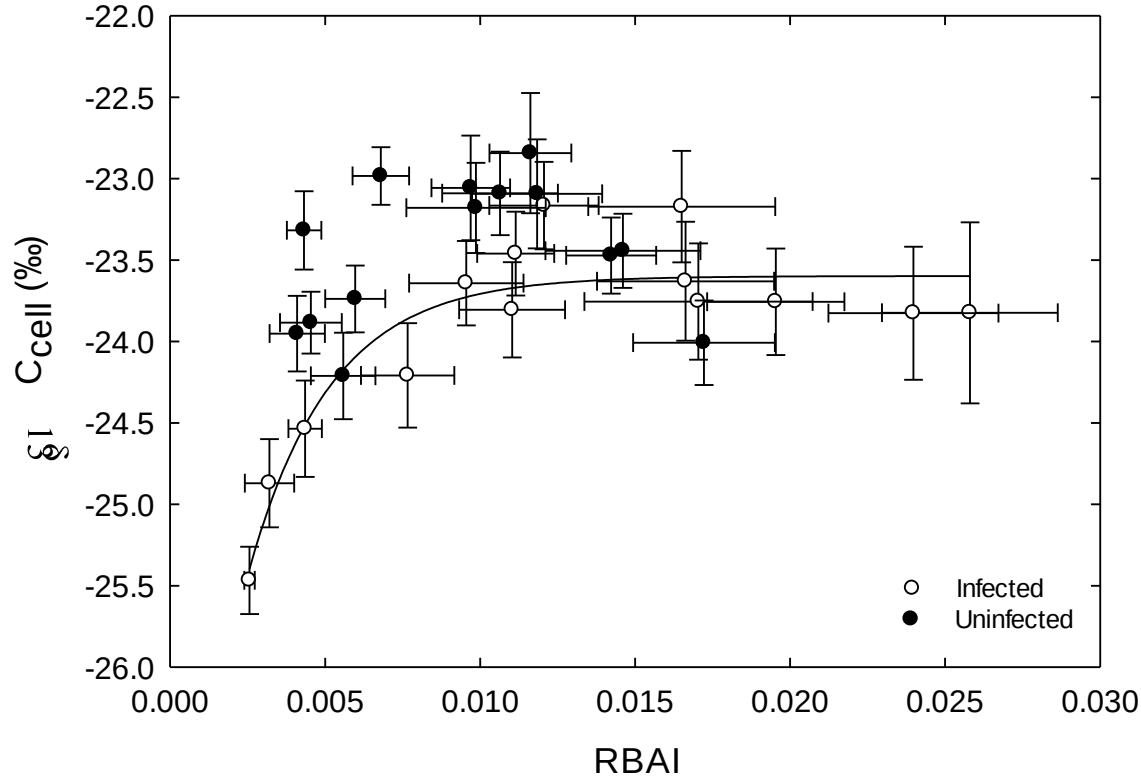

Figure 2. Mean ± SE of 5-year RBAI vs $\delta^{13}C_{cell}$ of uninfected (n=9) and infected trees (n=8) for the period 1876-1880 to 2006-2010. The $\delta^{13}C_{cell}$ of infected trees displayed an asymptotic relationship with RBAI described by a nonlinear exponential rise to a maximum ($P<0.0001$, $r^2 = 0.85$). No significant relationship was found between RBAI and $\delta^{13}C_{cell}$ of uninfected trees.

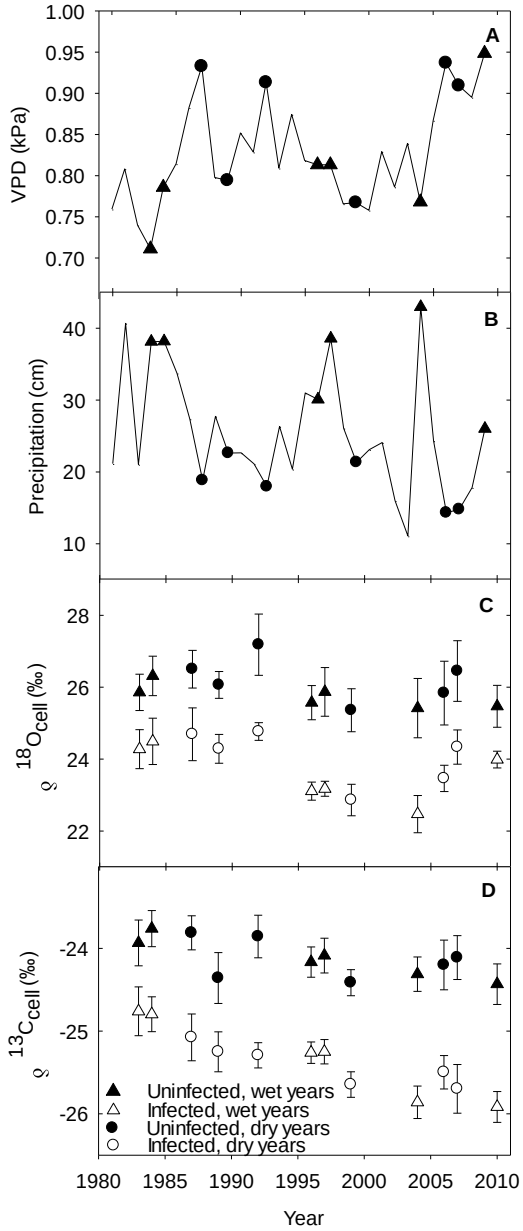

Figure 3. Daytime (0630-1930 h) vapor pressure deficit (VPD; **A**), and precipitation (**B**) during the growing season (DOY 121-274) at the Wind River Field Station for the period 1980-2010. Wet and dry years correspond with years selected for $\delta^{13}C_{cell}$ and $\delta^{18}O_{cell}$ analyses. Mean ± SE of (**C**) $\delta^{13}C_{cell}$ and (**D**) $\delta^{18}O_{cell}$ of two wet and two dry years per decade for the period 1980-2010 of uninfected and infected trees (n=6).

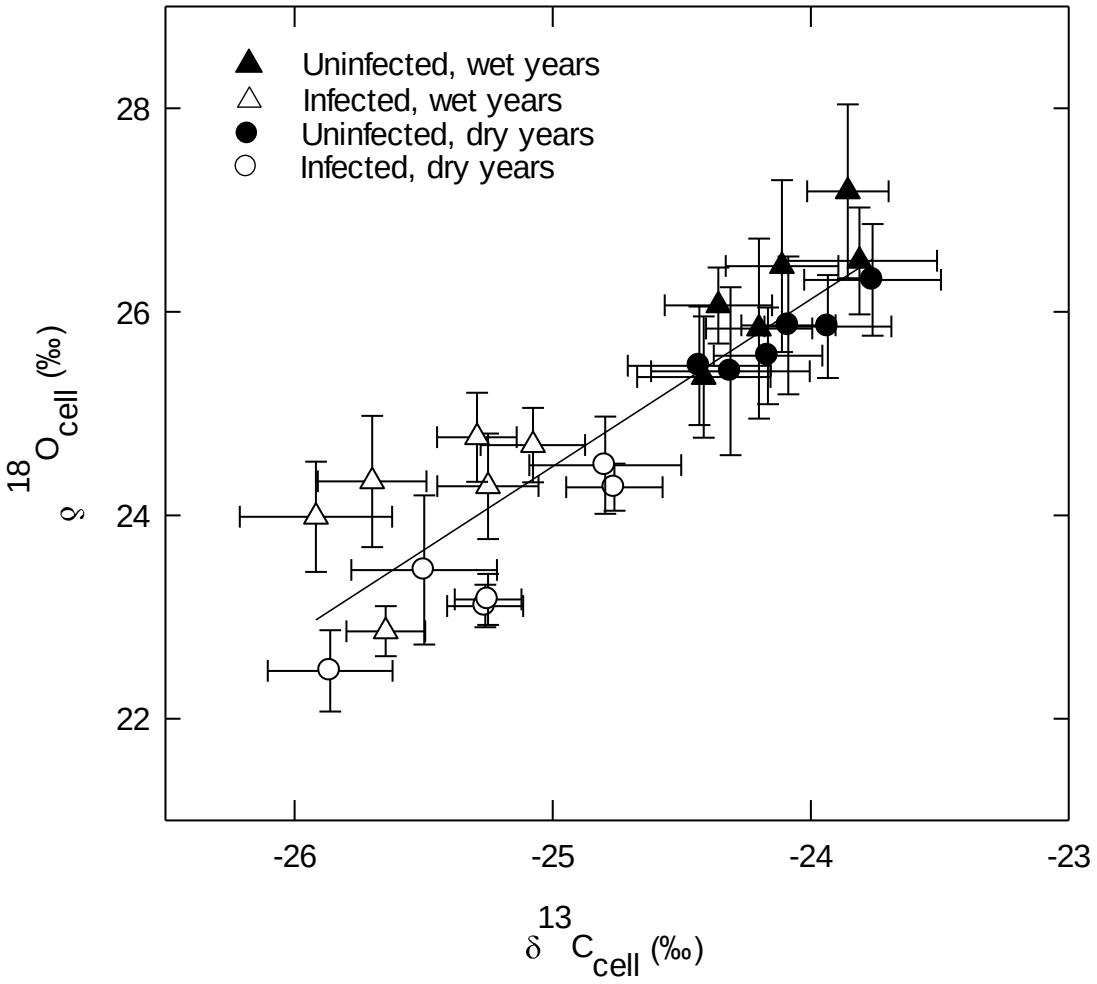

Figure 4. Mean ± SE $\delta^{13}C_{cell}$ vs $\delta^{18}O_{cell}$ of wet and dry years for the period 1980-2010 of uninfected and infected trees (n=6).

TABLES

Table 1. Stem diameter, age, and height of western hemlock trees uninfected and infected with dwarf mistletoe

	Diameter (cm)	Age (years)	Height (m)
Uninfected	91.3 ± 2.9 a	225 ± 31.3 a	52.1 ± 0.9 a
Infected	90.6 ± 4.6 a	210 ± 27.2 a	48.8 ± 1.5 a

Values are means (± SE) of measurements made in 2011. Values followed by different letters within each column differ significantly at $P \leq 0.05$; n=8-17.

Table 2. Parameters for *A*-c_i curves determined for western hemlock trees uninfected and infected with dwarf mistletoe and described by the equation $A = y_0 + a(1 - e^{-bx})$.

	Uninfected	Infected
y_0	-6.9602	-3.3173
a	35.7206	18.1075
b	0.0019	0.002

Table 3. Tree-ring $\delta^{13}C_{cell}$ and $\delta^{18}O_{cell}$, field measurements of $g_{s,}$ and estimates of g_m, and L of western hemlock trees uninfected and infected with dwarf mistletoe

Condition	$\delta^{13}C_{cell}$ (‰)	$\delta^{18}O_{cell}$ (‰)	g_s (mmol m^{-2} s^{-1})	g_m (mmol m^{-2} s^{-1})	L (m)
Uninfected	-24.4 ± 0.2 a	25.4 ± 0.6 a	29.2 ± 1.9 a	38.7 ± 0.003 a	0.12 ± 0.03 a
Infected	-25.6 ± 0.2 b	22.9 ± 0.2 b	33.4 ± 2.7 a	25.4 ± 0.003 b	0.35 ± 0.02 b

Values are means (± SE). Values followed by different letters within each column differ significantly at $P \leq 0.05$; n=3-6.

3. CONCLUSIONS

In this study, I used tree ring radial growth (quantified as relative basal area increment, RBAI) and C and O stable isotope ($\delta^{13}C_{cell}$ and $\delta^{18}O_{cell}$, respectively) analyses to evaluate the effects of dwarf mistletoe (*Arceuthobium tsugense*) on the physiology and gas exchange of host western hemlock (*Tsuga heterophylla*) through time. Unlike leafy mistletoe, dwarf mistletoe has diminutive shoots and is a slowly progressing infection that results in indirect effects on host functioning through hydraulic architecture and gas exchange, rather than direct effects through the interception of carbon (C) and water as in leafy mistletoes. As discussed below, the results of this study have implications for the use of tree ring isotopes to detect when host trees were infected with dwarf mistletoe, the application of the dual isotope approach to systems with pathogens, stand-level processes related to water and carbon cycling, responses to changing climate, and forest health and management.

Challenges still remain in quantifying the effects of dwarf mistletoe on host physiology as well as estimating when trees were initially infected. Measurements of host and parasite physiology such as stomatal conductance (g_s), photosynthesis (A), and transpiration (E) are limited to relatively short time scales and can shed light on the physiology of the host-parasite relationship close to or at the time of measurement. However, estimating when trees were initially infected is particularly difficult because host trees can be infected for several years during the latency phase without visible signs of infection. In addition, progression of the dwarf mistletoe infection and witches' broom formation occurs over decades. As a result, one goal of this study was to evaluate the use of tree ring growth and stable isotope analyses as tools to date the

onset and progression of mistletoe infections. Studies using tree ring stable isotopes in systems with pathogens aim to detect "signatures" of infections back in time (Simard *et al.*, 2012). However, in the case of dwarf mistletoe-infected western hemlock, it remains unclear if I can use isotope analyses to date the onset of the infections because $\delta^{13}C_{cell}$ was not significantly different between groups prior to 1996-2000 (Figure 1b). This is likely because lightly and moderately infected trees do not display reduced growth relative to uninfected trees (Shaw *et al.*, 2008) and presumably the effects of dwarf mistletoe on the physiology of infected trees would not be significant enough to be recorded in tree rings until trees became heavily infected. Therefore, there may be a threshold at which infected trees become severely infected and exhibit the physiological impacts of the dwarf mistletoe infection. Because tree ring and stable isotope analyses do not detect the "signature" of the infection until trees are severely infected, these tools cannot be used to determine exactly when trees were infected.

Nonetheless, the $\delta^{13}C_{cell}$ of infected trees appeared to be consistently lower than that of uninfected trees from 1916-1920 to 1946-1950. This pattern was likely due to initial effects of the infection on host physiology via reductions in host tree *N* content and A_{max}, in the absence of stomatal adjustments, which would have led to reduced $\delta^{13}C_{cell}$. During 1956-1960, the $\delta^{13}C_{cell}$ trajectory of infected trees converged with that of uninfected trees. This convergence coincided with the time periods (1956-1960, 1966-1970) when RBAI of infected trees was significantly greater than uninfected trees presumably due to the initial formation of witches' brooms. The

transient increase in RBAI coinciding with the convergence of $\delta^{13}C_{cell}$ trajectories suggests that the disruption of growth regulating hormones induced by dwarf mistletoe (Logan *et al.,* 2012) resulted in increased photosynthetic leaf area (and thus *A*) and decreased g_s on a leaf area basis. This increase in *A* and decrease in g_s would cause host intrinsic water use efficiency (WUE) defined as A/g_s to increase, c_c/c_a (the ratio of the concentration of CO_2 in the chloroplast stroma to that in the atmosphere) to decrease, and thus $\delta^{13}C_{cell}$ to increase, as observed around 1956-1960.

The concurrent analyses of radial growth (RBAI) and $\delta^{13}C_{cell}$ suggested that I could detect the progression of the infection's effects on host physiology. From 1876-1880 to 2006-2010, the rate of decline in RBAI was significantly greater in infected than uninfected trees and infected trees had significantly greater RBAI than uninfected trees during 1886-1890. This likely occurred because western hemlock trees that became heavily infected were larger and growing faster in the past, consistent with studies relating dwarf mistletoe success to host vigor (Bickford *et al.,* 2005; Shaw et al., 2005; Stanton, 2007; Sanguesa-Barreda *et al.,* 2012). RBAI was significantly greater during 1956-1960 and 1966-1970 presumably due to the transient increase in photosynthetic leaf area due to witches' broom formation and also resulting in transient increases in RBAI. As the infection progressed, dwarf mistletoe diverted and sequestered host *N*, further reducing host A_{max} and radial growth. An increase in the number of branch infections further reduced branch hydraulic conductivity, causing infected trees to shed needles downstream of infection-induced swellings to maintain leaf-specific conductivity (Meinzer *et al.,* 2004). The remaining needles were unable

to support the respiratory demands of the increased branch area of the witches' brooms resulting in branch dieback. Reduced A_{max} and similar g_s between groups (Figure S1) likely resulted in reduced $\delta^{13}C_{cell}$, observed during 1996-2000 and 2006-2010. This coincides with significantly lower RBAI in infected than uninfected trees in 2006-2010 due to the diminished A_{max}, increased needle loss, and accelerated branch dieback. The concurrent analyses of ring widths and $\delta^{13}C_{cell}$ was valuable for detecting the progression of the physiological shifts induced by the dwarf mistletoe infection in host trees, and thus the intensification of dwarf mistletoe in tree crowns over time.

As discussed in Chapters 1 and 2, tree ring $\delta^{13}C_{cell}$ and $\delta^{18}O_{cell}$ can be used to infer tree responses to environmental conditions and forest pathogens. However, the dual isotope approach (Scheidegger *et al.,* 2000) is based on assumptions that are often not met under natural conditions and should be applied with caution (Roden & Siegwolf, 2012; Roden & Farquhar, 2012). Unlike leafy mistletoes that directly influence host water and C balance through interception of water and carbohydrates, the indirect impacts of the dwarf mistletoe infection on host branch hydraulic architecture and gas exchange made interpretations of $\delta^{13}C_{cell}$ and $\delta^{18}O_{cell}$ complex and challenging. I had expected infected trees to have similar $\delta^{18}O_{cell}$ to uninfected trees because previous measurements of leaf-specific hydraulic conductivity, g_s, and therefore transpiration on a unit leaf area basis were similar between groups (Meinzer *et al.,* 2004). However, the unexpected $\delta^{18}O_{cell}$ results in this study, which could not be explained by differences in environmental conditions or g_s alone, complicated

interpretations of the effects of the infection on host physiology. The surprising results shifted the focus of the study to other factors that could influence $\delta^{18}O_{cell}$ including the parameters *L* (effective pathlength) and g_m (mesophyll conductance). *L* and g_m are related to leaf anatomical characteristics and are known to influence $\delta^{13}C_{cell}$ and $\delta^{18}O_{cell}$ (Kahmen *et al.*, 2008; Seibt *et al.*, 2008; Song *et al.*, 2013) but are not incorporated or considered when applying the traditional dual isotope approach to infer relative changes in *A* and g_s. This is partially because g_m cannot be estimated retrospectively without field measurements of *A* (which were available in this case) and because *L* is impossible to measure and is only estimated using the Craig-Gordon Péclet model (Song *et al.*, 2013). In addition, it is difficult to incorporate these parameters into photosynthesis and leaf water O isotope models due to the lack of sufficient knowledge about species-specific patterns and the mechanisms involved in their regulation (Kahmen *et al.*, 2008; Seibt *et al.*, 2008; Flexas *et al.*, 2012; Song *et al.*, 2013). Interpretations of $\delta^{13}C_{cell}$ are complicated if g_s and g_m are not correlated (Lambers *et al.*, 2008, Seibt *et al*. 2008) because shifts in g_m can lead to changes in the ratio of CO_2 concentration in the chloroplast stroma (c_c) to that of the atmosphere (c_a) (represented as c_c/c_a) that are not directly included in the photosynthetic C isotope discrimination model where c_i/c_a (the ratio of CO_2 concentration of intercellular spaces (c_i) to c_a) is used instead (Farquhar *et al*., 1982). This variation can be large enough to account for variations in $\delta^{13}C_{leaf}$ and thus $\delta^{13}C_{cell}$ (Seibt *et al*., 2008). Therefore g_m and its relative contribution to the limitation of A_{max} and its co-regulation with g_s must be considered when interpreting $\delta^{13}C_{cell}$ and WUE, often used to predict

how plants may respond to future shifts in climate (Sanguesa-Barreda *et al.,* 2012). Further investigation of the relationship between L and g_m can improve interpretations of $\delta^{13}C_{cell}$ and $\delta^{18}O_{cell}$. Because dwarf mistletoe had significant impacts on co-occurring uninfected and infected western hemlock in this study, it is clear that undetected pathogens like dwarf mistletoe influence leaf-level gas exchange and complicate the use of tree ring stable isotopes for reconstructions of climate and tree responses to climatic variables.

In addition to L and g_m, the time spent at isotopic steady state was also considered as a factor that might explain the observed $\delta^{18}O_{cell}$ patterns. Isotopic steady state indicates that the isotopic composition of water entering the leaf from the xylem is the same as that of water evaporating from the leaf (Lai *et al.,* 2005). Steady state approaches accurately describe leaf water isotopic enrichment for long time periods such as months, years, or larger spatial scales (Werner *et al*., 2012). However, studies show that the assumption of steady state is often not met in natural conditions and as a result, has substantial effects on diurnal measurements of $\delta^{18}O$ of leaf water ($\delta^{18}O_{lw}$) and thus $\delta^{18}O_{cell}$ (Farquhar & Cernusak, 2005; Lai *et al*. 2006, Cuntz *et al*., 2007). In this study, I could not model non-steady state estimates of $\delta^{18}O_{lw}$ and $\delta^{18}O_{cell}$ based on annual tree ring cellulose because at least two or more diurnal measurements of $\delta^{18}O_{lw}$ are required (Farquhar & Cernusak, 2005). Because diurnal g_s did not differ between groups (Appendix C), leaf water residence times should also not have differed and therefore, the amount of mixing between unenriched xylem water and enriched water at evaporative sites should not have differed significantly between groups. As a result,

I was able to rule out isotopic state as a factor driving the observed differences in $\delta^{18}O_{cell}$ between groups. However, similar to L and g_m, isotopic state is often ignored in models although there is evidence that it can have substantial effects on leaf water and thus $\delta^{18}O_{cell}$.

This may be the first study involving the dual isotope approach, tree ring isotopes, and a forest pathogen to consider dwarf mistletoe's effects on leaf anatomical characteristics that are related to L and g_m. Dwarf mistletoe's indirect effects on host physiology rather than direct effects of other pathogens (e.g. leafy mistletoes intercepting water; insects feeding on phloem and leaf tissue) make dwarf mistletoe a unique system to employ the dual isotope approach, Craig-Gordon Péclet model, and estimates of L and g_m to interpret the nature of mistletoe-induced alterations in host photosynthetic gas exchange. Using this approach on other species of dwarf mistletoe-host systems and under different climatic conditions—such as water-limited locations—will be useful for broadening the application of tree ring isotopes to infer effects of pathogens, which may become more widespread with future climate shifts (Hennon *et al.,* 2011). To confirm my findings that L and g_m were likely driving changes in $\delta^{18}O_{cell}$, studies of dwarf mistletoe's effects on host leaf anatomy would be prudent.

Despite its small size relative to host western hemlock trees, dwarf mistletoe-induced shifts in leaf-level gas exchange influence whole trees and thus entire stands. The increased N demand associated with the infection significantly reduced the N content and photosynthetic capacity (A_{max}) of host trees (Meinzer *et al.,* 2004). Since

water use of infected trees was 40% lower than uninfected trees, estimated photosynthesis was reduced by 21%, and transpiration rates per unit leaf area were similar between groups, an estimated total C accumulation by infected trees was likely reduced by about 60% (Meinzer *et al.*, 2004). Lower water use in infected trees implies that more water will remain in the soil and be available for uninfected trees. In addition, a stand with a high percentage of heavily infected trees that occupy the same area as healthy trees will have lower evapotranspiration than stands without infected trees because of dramatically reduced leaf area per infected tree (Meinzer *et al.*, 2004). Needle loss and branch dieback caused by the infection would increase standing dead wood and downed wood that could increase the amount of C released from the stand. It is clear that scaling between tree and stand level processes related to water and C fluxes should include measurements from both uninfected and infected trees because a 60% reduction in C accumulation on a per tree basis, for example, can significantly influence the C balance of entire stands that contain an appreciable fraction of heavily infected trees.

Climate strongly influences where tree species and their associated pathogens can survive. Because dwarf mistletoe has substantial effects at the leaf, whole tree, and stand level, this study has implications for how infected trees and stands respond to changing climate such as drought, increasing atmospheric CO_2 concentrations, and surface temperature (Way, 2011). Hennon *et al*. (2011) found that *A. tsugense* was concentrated at low elevations, where there are longer growing seasons required for fruit maturation and seed dispersal as well as less snow that could cause over-

wintering seeds to slough off of western hemlock branches. Because longer growing seasons and reduced snowfall are among climate predictions for the geographical range of western hemlock (IPCC 2007), dwarf mistletoe may be favored by a warmer climate and increase its range and impact on host western hemlock.

Studies have suggested that dwarf mistletoe-infected trees may be more susceptible to other pests or extreme climate events like drought that may increase tree mortality (Kenaley *et al.*, 2008; Way, 2011). Host trees infected with dwarf mistletoe in water-limited locations may also respond differently to climate. Observations of Geils *et al.* (2002) suggested that damage to host ponderosa pine is more severe in the drier parts of its distribution with the most severely infested stands located in the eastern Sierra and Cascade forests. This observation coincides with recent studies documenting widespread forest mortality that has been attributed to a combination of increasing drought severity, surface temperatures, and prevalence of insects and pathogens (McDowell *et al*., 2008; Allen *et al*., 2009; van Mantgem *et al.*, 2009). Therefore, investigating the effect of dwarf mistletoe on host species in relatively drier climates will inform host responses to infection during water stress, as well as the physiological mechanisms of forest mortality, which remain unresolved. Conklin (2003) found that host mortality that was strongly correlated with dwarf mistletoe infection was also greatly influenced by drought. Stanton (2007) conducted a tree ring growth and climate sensitivity analysis and found that host ponderosa pine (*Pinus ponderosa*) infected with *A. vaginatum* was more sensitive to climate than uninfected trees. However, both uninfected and infected western hemlock ring widths, $\delta^{13}C_{cell}$,

and $\delta^{18}O_{cell}$ were not correlated with climate variables (Appendices B, D). This contrast between ponderosa pine and western hemlock infected with dwarf mistletoe is likely due to host responses to differences in water availability. Sanguesa-Barreda *et al*. (2012) used tree ring $\delta^{13}C_{cell}$ to investigate the interactions of leafy mistletoe infection, rising atmospheric CO_2 concentrations and drought on WUE of host Scots pine. They hypothesized that WUE would increase with increasing CO_2 concentrations. They concluded that the growth of infected trees was more sensitive to drought stress than uninfected trees and that the combined effect of drought stress and mistletoe infection caused a reduction in growth and reversed the CO_2-induced increase in WUE. Similarly, lower $\delta^{13}C_{cell}$ of infected western hemlock trees suggested that infected trees had lower WUE and may be a smaller C sink than uninfected trees despite increasing atmospheric CO_2 concentrations (Keeling *et al.,* 1995). Because the physiological effects of dwarf mistletoe on its host remain unresolved and vary across dwarf mistletoe-host species (Meinzer *et al.,* 2004; Sala *et al.,* 2001; Logan *et al.,* 2002), studies of different dwarf mistletoe and host species from different climates will improve our understanding of the system and the range of species-specific responses to disturbance and stress, including drought and pests (Kenaley *et al*., 2008).

Studies integrating leaf to whole-tree physiology will improve our understanding of this system from the tree to canopy scale and better inform forest management decisions, especially since dwarf mistletoe is observed to have ecosystem-scale effects that are still being explored (Watson, 2001; Shaw *et al*., 2004; Bell & Adams, 2011; Way, 2011). Birds, mammals, and insects use dwarf mistletoe

seeds and induced witches' brooms as a food source and microhabitat, making dwarf mistletoe ecologically valuable (Watson, 2001). Dwarf mistletoe also influences C and water balance, nutrient transfer through litter fall, and fire regimes in stands, as witches' brooms often increase susceptibility to fire. Spatial patterns of uninfected and infected trees influence understory succession as well as the amount of sunlight that reaches understory vegetation and wildlife. Because dwarf mistletoe management efforts require a balance between pest impacts and ecological benefits, management of this system is complex. A better understanding of the physiological effects of different dwarf mistletoe-host systems will inform ecosystem management efforts.

REFERENCES

Allen CD, Macalady AK, Chenchouni H, Bachelet D, McDowell N, Vennetier M, Kitzberger T, Rigling A, Breshears DD, Hogg EH, Gonzalez P, Fensham R, Zhang Z, Castro J, Demidova N, Lim J-H, Allard G, Running SW, Semerci A, Cobb N. 2010. A global overview of drought and heat-induced tree mortality reveals emerging climate change risks for forests. *Forest Ecology and Management* 259: 660-684.

Bell TL, Adams MA. 2011. Attack on all fronts: functional relationships between aerial and root parasitic plants and their woody hosts and consequences for ecosystems. *Tree Physiology* 31:3-15.

Bickford CP, Kolb TE, Geils BW. 2005. Host physiological condition regulates parasitic plant performance: *Arceuthobium vaginatum* subsp. *cryptopodum* on *Pinus ponderosa*. *Oecologia* 146: 179–189.

Conklin DA. 2003. Comparison of dwarf mistletoe behavior and stand development in treated and untreated areas: 10-year monitoring on Jarita Mesa. USDA Forest Service, Southwestern Region Forestry and Forest Health Report R3-03-02. Albuquerque, NM, 11p.

Cuntz M, Ogee J, Farquhar GD, Peylin P and Cernusak LA. 2007. Modelling advection and diffusion of water isotopologues in leaves. *Plant, Cell & Environment* 30: 892–909.

Farquhar GD and Cernusak LA. 2005. On the isotopic composition of leaf water in the non-steady state. *Functional plant biology* 32: 293-303.

Flexas J, Barbour MM, Brendel O, Cabrera HM, Carriquí M, Diaz-Espejo A, Douthe C, Dreyer E, Ferrio JP, Gago J, Galle A, Galmes J, Kodama N, Medano H, Niinemets U, Pequero-Pina JJ, Pou A, Ribas-Carbo M, Tomas M, Tosens T, Warren CR. 2012. Mesophyll diffusion conductance to CO2: An unappreciated central player in photosynthesis. *Plant Science* 196: 70-84.

Geils BW, Tovar JC, Moody B. **2002**. Mistletoes of North American Conifers. General Technical Report RMRS-GTR-98.

Hennon, P, Barrett TM, Wittwer D. 2011. "The distribution of hemlock dwarf mistletoe suggests influences of climate," *Forests of Southeast and South-Central Alaska, 2004-2008*. Gen. Tech. Rep. PNW-GTR-835. Portland, OR: U.S. Department of Agriculture, Forest Service, Pacific Northwest Research Station, pp. 74-77.

IPCC, 2007: Climate Change 2007: The Physical Science Basis. Contribution of Working Group I to the Fourth Assessment Report of the Intergovernmental Panel on Climate Change [Solomon, S., D. Qin, M. Manning, Z. Chen, M. Marquis, K.B. Averyt, M.Tignor and H.L. Miller (eds.)]. Cambridge University Press, Cambridge, United Kingdom and New York, NY, USA.

Kahmen A, Simonin K, Tu KP, Merchant A, Callister A, Siegwolf R, Dawson TE, Arndt SK. 2008. Effects of environmental parameters, leaf physiological properties and leaf water relations on leaf water δ18O enrichment in different Eucalyptus species. *Plant, cell & environment* 31: 738-751.

Keeling, CD, Whorf TP, Wahlen M, Licht JVD. 1995. Interannual extremes in the rate of rise of atmospheric carbon dioxide since 1980. *Nature* 375: 666-670.

Kenaley S, Mathiasen R, James HE. 2008. Mortality associated with a bark beetle outbreak in dwarf mistletoe-infested ponderosa pine stands in Arizona. *Western Journal of Applied Forestry* 23: 112-120.

Lai CT, Ehleringer JR, Bond BJ, Tha Paw UK. 2006. Contributions of evaporation, isotopic non-steady state transpiration and atmospheric mixing on the δ18O of water vapour in the Pacific Northwest coniferous forests. *Plant, Cell & Environment* 29: 77-94.

Lambers H, Chapin FS, Chapin FS, Pons TL. 2008. *Plant physiological ecology*. New York, US: Springer.

Logan BA, Huhn ER, Tissue DT. 2002. Photosynthetic characteristics of eastern dwarf mistletoe (*Arceuthobium pusillum* Peck) and its effects on the needles of host white spruce (*Picea glauca* [Moench] Voss). *Plant Biology* 4: 740-745.

Logan BA, Reblin JS, Zonana DS, Dunlavey RF, Hricko CR, Hall AW, Schmiege SC, Buschek RA, Duran KL, Neil Emery RJ, Kurepin LV, Lewis JD, Pharis RP, Phillips NH, Tissue DT. 2012. Impact of eastern dwarf mistletoe (*Arceuthobium pusillum*) on host white spruce (*Picea glauca*) development, growth and performance across multiple scales. *Physiologia Plantarum* 147: 502–513.

McDowell N, Pockman WT, Allen CD, Breshears DD, Cobb N, Kolb T, Plaut J, Sperry J, West A, Williams DG, Yepez EA. 2008. Mechanisms of plant survival and mortality during drought: why do some plants survive while others succumb to drought? *New Phytologist* 178: 719-739.

Meinzer FC, Woodruff DR, Shaw DC. 2004. Integrated responses of hydraulic architecture, water and carbon relations of western hemlock to dwarf mistletoe infection. *Plant, Cell and Environment* 27:937-946.

Roden & Siegwolf. 2012. Is the dual-isotope conceptual model fully operational? *Tree physiology* 32: 1179-1182.

Roden JS, Farquhar GD. 2012. A controlled test of the dual-isotope approach for the interpretation of stable carbon and oxygen isotope ratio variation in tree rings. *Tree Physiology* 4: 490-503.

Sala A, Carey EV, Callaway RM. 2001. Dwarf mistletoe affects whole-tree water relations of Douglas fir and western larch primarily through changes in leaf to sapwood ratios. *Oecologia* 126: 42-52.

Sanguesa-Barreda G, Linares JC, Camarero JJ. 2013. Drought and mistletoe reduce growth and water-use efficiency of Scots pine. *Forest Ecology and Management* 296: 64-73.

Scheidegger Y, Saurer M, Bahn M, Siegwolf R. 2000. Linking stable oxygen and carbon stable isotopes with stomatal conductance and photosynthetic capacity: a conceptual model. *Oecologia* 125: 350-357.

Schulze ED, Turner NC, Glatzel G. 1984. Carbon, water and nutrient relations of two mistletoes and their hosts: A hypothesis. *Plant, Cell and Environment* 7: 293-299.

Seibt U, Rajabi A, Griffiths H, Berry JA. 2008. Carbon isotopes and water use efficiency: sense and sensitivity. *Oecologia* 155: 441–454.

Shaw DC, Watson DM, Mathiasen RL. 2004. Comparison of dwarf mistletoes (*Arceuthobium spp., Viscaceae*) in the western United States with mistletoes (*Amyema spp., Loranthaceae*) in Australia--ecological analogs and reciprocal models for ecosystem management. *Australian Journal of Botany* 52:481-498.

Shaw DC, Chen J, Freeman EA, Braun DM. 2005. Spatial and population characteristics of dwarf mistletoe infected tree sin an old-growth Douglas-fir – western hemlock forest. *Canadian Journal of Forest Research* 35: 990-1001.

Simard S, Morin H, Krause C, Buhay WM, Treydte K. 2012. Tree-ring widths and isotopes of artificially defoliated balsam firs: A simulation of spruce budworm outbreaks in Eastern Canada. *Environmental and Experimental Botany* 81: 44-54.

Song X, Barbour MM, Farquhar GD, Vann DR, Helliker BR. 2013. Transpiration rate relates to within- and across- species variations in effective pathlength in a leaf water model of oxygen isotope enrichment. *Plant, Cell & Environment*. doi: 10.1111/pce.12063.

Stanton S. 2007. Effects of dwarf mistletoe on climate response of mature ponderosa pine trees. *Tree-Ring Research* 63: 69-80.

Van Mantgem PJ, Stephenson NL, Byrne JC, Daniels LD, Franklin JF, Fule PZ, Harmon ME, et al. 2009. Widespread increase of tree mortality rates in the western United States. *Science* 323: 521-524.

Watson DM. 2001. Mistletoe--A Keystone Resource in Forests and Woodlands Worldwide. *Annual Review of Ecology and Systematics* 32:219-249.

Way D. 2011. Parasitic plants and forests: a climate change perspective. *Tree Physiology* 31:1-2.

Werner C, Schnyder H, Cuntz M, Keitel C, Zeeman MJ, Dawson TE, Badeck F-W, Brugnoli E, Ghashghaie J, Grams TEE, Kayler ZE, Lakatos M, Lee X, Maguas C, Ogee J, Rascher KG, Siegwolf RTW, Unger S, Welker J, Wingate L, Gessler A. 2012. Progress and challenges in using stable isotopes to trace plant carbon and water relations across scales. *Biogeosciences* 9: 3083-3111.

APPENDICES

Appendix A. Daytime climate conditions during the growing season in 1999 and 2002.

Year	T_{air} (ºC)	RH (%)	VPD (kPa)	Precipitation (cm)
1999	17.1	60.6	0.77	21.3
2002	17.6	60.8	0.79	16.0

Appendix B. Correlation (top values) and significance levels (bottom values) of the regressions between ring widths and climate variables: minimum and maximum temperature, precipitation, and PDSI for uninfected (**A**) and infected (**B**) trees. Bolded values are significant at P≤0.05; n=13-17. Correlation analyses based on Pearson's correlation coefficients were performed with MS Excel Data Solver package for 1895-1950 and 1951-2010.

(A)

Infected	Period	Jan	Feb	Mar	Apr	May	Jun	Jul	Aug	Sep	Oct	Nov	Dec
Min temperature	1895-1950	-0.16	0.12	**0.34**	0.19	-0.20	-0.20	-0.19	-0.08	-0.09	0.07	0.07	-0.18
		0.24	0.36	**0.01**	0.17	0.14	0.13	0.16	0.54	0.51	0.63	0.60	0.20
	1951-2010	0.17	0.31	0.10	-0.13	-0.03	0.05	-0.02	0.14	0.00	-0.03	0.23	0.05
		0.18	0.02	0.45	0.34	0.82	0.72	0.86	0.30	0.98	0.85	0.08	0.69
	1895-2010	0.03	0.21	**0.20**	0.01	-0.09	-0.03	-0.06	0.07	-0.02	0.02	0.17	-0.05
		0.77	0.02	**0.03**	0.93	0.32	0.78	0.52	0.43	0.79	0.86	0.06	0.57
Max temperature	1895-1950	-0.20	0.14	0.28	-0.01	-0.04	-0.11	-0.17	-0.12	0.01	-0.05	-0.19	-0.21
		0.15	0.29	0.36	0.92	0.76	0.40	0.21	0.38	0.97	0.73	0.15	0.13
	1951-2010	0.21	0.24	0.12	-0.26	-0.14	**-0.28**	-0.16	0.01	-0.14	0.02	0.13	0.04
		0.11	0.06	0.35	0.05	0.27	**0.03**	0.22	0.96	0.30	0.85	0.30	0.76
	1895-2010	0.05	**0.06**	**0.15**	-0.06	-0.03	**-0.14**	-0.16	-0.07	-0.14	-0.12	-0.05	-0.08
		0.78	**0.03**	**0.04**	0.12	0.29	**0.03**	0.10	0.75	0.50	0.97	0.91	0.46
Precipitation	1895-1950	0.00	0.00	-0.01	0.20	-0.08	0.20	0.27	-0.10	0.05	0.22	0.15	-0.24
		0.99	0.97	0.94	0.13	0.58	0.14	0.04	0.48	0.71	0.10	0.29	0.08
	1951-2010	0.05	0.01	-0.20	0.04	0.02	0.08	0.12	-0.05	-0.06	-0.27	0.20	0.04
		0.72	0.93	0.12	0.79	0.88	0.53	0.37	0.72	0.65	0.04	0.13	0.77
	1895-2010	0.04	0.00	-0.11	0.11	-0.03	0.14	0.18	-0.06	-0.02	-0.07	0.17	-0.09
		0.68	0.97	0.25	0.25	0.74	0.14	0.05	0.56	0.87	0.49	0.07	0.34
PDSI	1895-1950	0.02	-0.02	-0.03	0.12	0.06	0.17	0.20	0.10	0.04	0.17	0.15	0.01
		0.87	0.88	0.81	0.39	0.66	0.21	0.14	0.44	0.75	0.22	0.27	0.93
	1951-2010	0.12	0.09	0.00	0.16	0.15	0.20	0.19	0.19	0.15	0.00	0.17	0.12
		0.35	0.48	0.98	0.22	0.25	0.12	0.15	0.16	0.25	0.99	0.18	0.34
	1895-2010	0.09	0.06	0.00	0.15	0.12	**0.19**	**0.20**	0.16	0.11	0.07	0.17	0.08
		0.31	0.55	0.99	0.11	0.20	**0.04**	**0.03**	0.09	0.22	0.44	0.07	0.37

(B)

Uninfected	Period	Jan	Feb	Mar	Apr	May	Jun	Jul	Aug	Sep	Oct	Nov	Dec
Min temperature	1895-1950	-0.13 0.33	0.17 0.21	**0.34** **0.01**	0.07 0.59	-0.11 0.40	-0.23 0.09	-0.40 0.00	-0.14 0.30	-0.17 0.22	0.06 0.64	0.09 0.49	-0.11 0.44
	1951-2010	0.15 0.24	0.28 0.03	0.10 0.47	0.00 0.98	-0.03 0.80	0.06 0.64	0.14 0.29	0.24 0.07	0.09 0.48	0.00 0.99	0.14 0.29	-0.05 0.70
	1895-2010	0.00 1.00	0.17 0.07	0.17 0.08	0.03 0.76	-0.08 0.40	-0.07 0.47	-0.08 0.41	0.06 0.54	-0.01 0.94	0.02 0.81	0.10 0.31	-0.07 0.44
Max temperature	1895-1950	-0.08 0.57	0.14 0.29	0.17 0.20	-0.08 0.58	-0.03 0.85	-0.02 0.88	**-0.32** **0.02**	-0.13 0.36	-0.12 0.37	-0.18 0.18	-0.19 0.15	-0.12 0.39
	1951-2010	0.20 0.12	0.05 0.68	0.16 0.23	-0.09 0.49	-0.02 0.86	-0.18 0.16	-0.04 0.76	-0.01 0.95	-0.12 0.35	-0.07 0.60	0.08 0.53	-0.04 0.78
	1895-2010	0.05 0.61	0.06 0.52	0.15 0.10	-0.06 0.51	-0.03 0.75	-0.14 0.12	-0.16 0.10	-0.07 0.45	-0.14 0.14	-0.12 0.21	-0.05 0.63	-0.08 0.42
Precipitation	1895-1950	0.10 0.46	0.15 0.28	0.10 0.48	0.24 0.08	-0.08 0.57	0.06 0.67	0.20 0.15	-0.08 0.55	0.18 0.17	0.33 0.01	0.13 0.33	-0.18 0.18
	1951-2010	-0.01 0.93	0.19 0.14	-0.22 0.09	0.09 0.50	-0.04 0.78	0.00 0.98	0.14 0.30	-0.07 0.60	0.05 0.71	-0.08 0.57	0.20 0.12	0.02 0.87
	1895-2010	0.01 0.92	0.17 0.07	-0.09 0.36	0.13 0.16	-0.04 0.64	0.02 0.87	0.16 0.09	-0.09 0.34	0.11 0.23	0.06 0.49	0.17 0.07	-0.07 0.46
PDSI	1895-1950	0.09 0.52	0.10 0.47	0.12 0.40	0.25 0.06	0.08 0.56	0.12 0.39	0.14 0.32	0.13 0.35	0.13 0.34	0.23 0.09	0.17 0.21	0.07 0.60
	1951-2010	0.19 0.14	0.25 0.06	0.10 0.44	0.16 0.22	0.12 0.35	0.13 0.31	0.14 0.27	0.14 0.30	0.11 0.39	0.04 0.74	0.15 0.25	0.12 0.36
	1895-2010	0.12 0.20	0.17 0.06	0.08 0.41	0.15 0.11	0.07 0.45	0.09 0.34	0.11 0.26	0.10 0.28	0.09 0.31	0.09 0.33	0.13 0.16	0.07 0.45

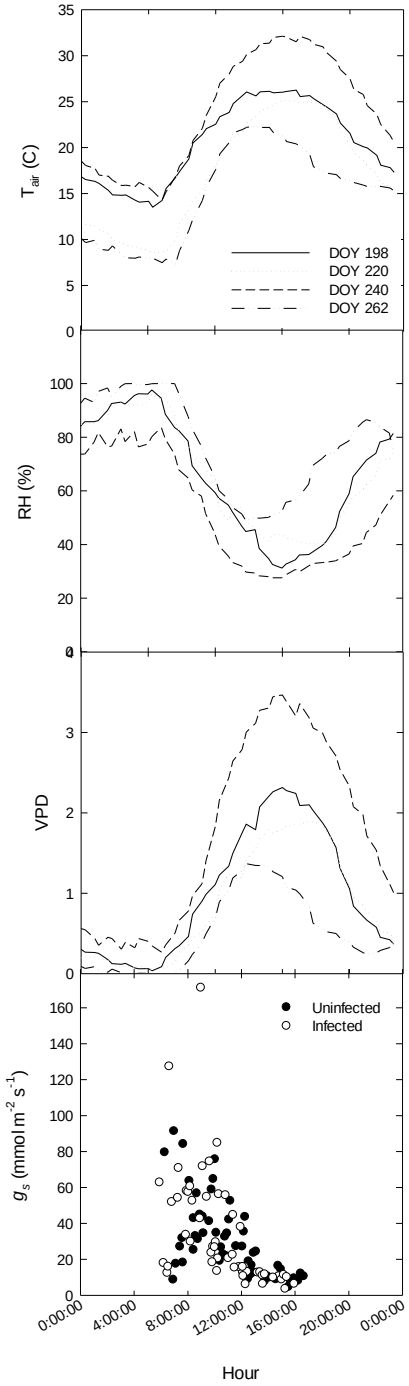

Appendix C. Diurnal time courses of T_{air}, RH, VPD, and g_s on four dates during the 2002 growing season on three branches of uninfected and infected trees (n=3).

Appendix D. Correlation coefficients (top values) and significance levels (bottom values) of the regressions of $\delta^{13}C_{cell}$ and $\delta^{18}O_{cell}$ vs. climate variables: T_{air}, RH, total growing season precipitation, and VPD for the period 1980-2010; n=6.

Condition		T_{air}	RH	Precipitation	VPD
Uninfected	$\delta^{13}C_{cell}$	0.21 0.50	-0.19 0.55	-0.09 0.79	0.22 0.49
Infected	$\delta^{13}C_{cell}$	-0.25 0.43	0.20 0.53	0.057 0.86	-0.22 0.49
Uninfected	$\delta^{18}O_{cell}$	-0.16 0.62	-0.13 0.70	-0.22 0.50	0.01 0.99
Infected	$\delta^{18}O_{cell}$	0.23 0.48	-0.44 0.15	-0.32 0.31	0.37 0.23

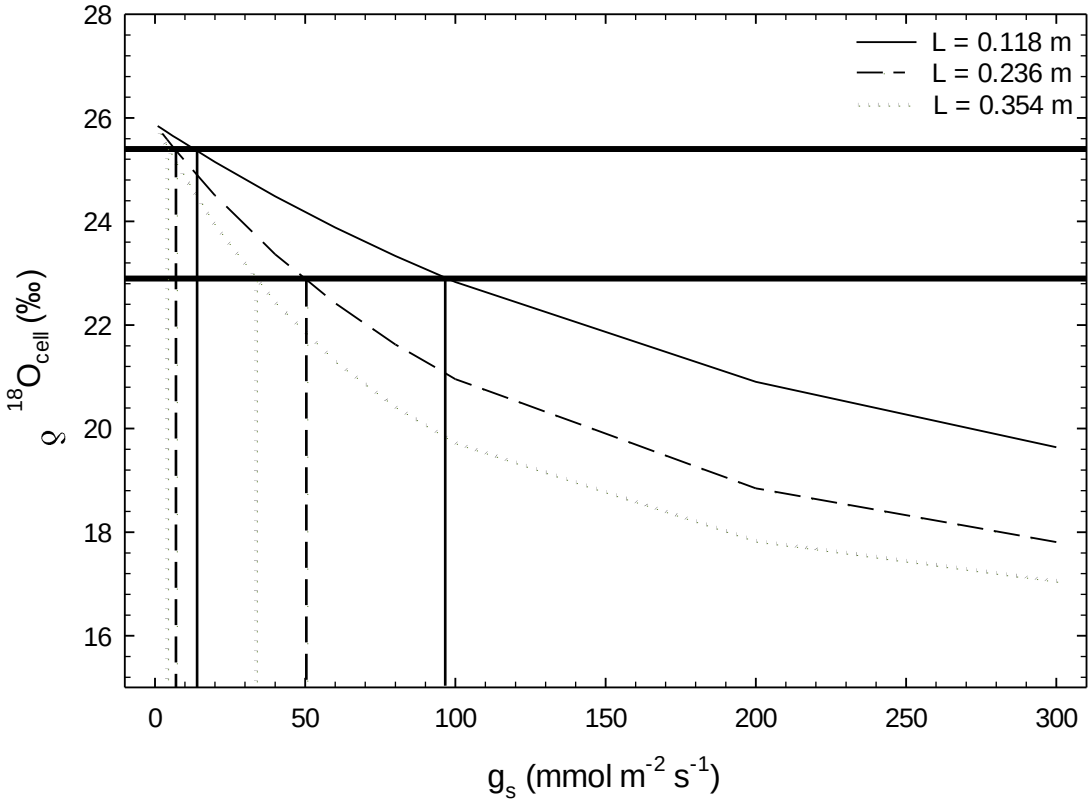

Appendix E. Sensitivity analysis using the Craig-Gordon Péclet model to compare g_s and $\delta^{18}O_{cell}$ at constant values of L of uninfected (L=0.118 m), infected (L=0.354 m), and the average of both groups (L=0.236 m). Horizontal lines represent observed $\delta^{18}O_{cell}$ values of 1999 tree rings for uninfected (25.5‰) and infected (22.9‰) trees. Vertical lines represent the values of g_s that would result in the observed $\delta^{18}O_{cell}$ values of uninfected and infected trees for the different values of L.